AWARD NUMBER: W81XWH-22-1-0094

TITLE: Defining Cardiac Innervation and Reinnervation During Cardiac Injury

PRINCIPAL INVESTIGATOR: Ahmed Mahmoud

CONTRACTING ORGANIZATION: University of Wisconsin System, Madison, WI

REPORT DATE: May 2023

TYPE OF REPORT: Annual

PREPARED FOR: U.S. Army Medical Research and Development Command
Fort Detrick, Maryland 21702-5012

DISTRIBUTION STATEMENT: Approved for Public Release;
Distribution Unlimited

REPORT DOCUMENTATION PAGE

Form Approved
OMB No. 0704-0188

1. REPORT DATE	**2. REPORT TYPE**	**3. DATES COVERED**
May 2023	Annual	15Apr2022-14Apr2023

4. TITLE AND SUBTITLE

Defining Cardiac Innervation and Reinnervation During Cardiac Injury

5a. CONTRACT NUMBER
W81XWH-22-1-0094

5b. GRANT NUMBER

5c. PROGRAM ELEMENT NUMBER

6. AUTHOR(S)

Ahmed Mahmoud, PhD

E-Mail: aimahmoud@wisc.edu

5d. PROJECT NUMBER

5e. TASK NUMBER

5f. WORK UNIT NUMBER

7. PERFORMING ORGANIZATION NAME(S) AND ADDRESS(ES)

UNI VERSITY OF WISCONSIN SYSTEM
RESEARCH AND SPONSORED PROGRAMS
BOARD OF REGENTS
21 N PARK ST STE 6301
MADISON WI 53715-1218

8. PERFORMING ORGANIZATION REPORT NUMBER

9. SPONSORING / MONITORING AGENCY NAME(S) AND ADDRESS(ES)

U.S. Army Medical Research and Development Command
Fort Detrick, Maryland 21702-5012

10. SPONSOR/MONITOR'S ACRONYM(S)

11. SPONSOR/MONITOR'S REPORT NUMBER(S)

12. DISTRIBUTION / AVAILABILITY STATEMENT

Approved for Public Release; Distribution Unlimited

13. SUPPLEMENTARY NOTES

14. ABSTRACT

Cardiac nerves regulate essential roles in development, homeostasis, and repair. Yet, the precise architecture of the intact, cardiac nervous system has not been rigorously analyzed. Our goal is to model the intact, mammalian cardiac nervous system and neurovascular network in high-resolution using lineage tracing, tissue clearing, whole-mount imaging, and 3D modeling. Excitingly, our results identify extensive parasympathetic innervation in the cardiac ventricles, challenging the clinical misconception that parasympathetic nerves only innervate the cardiac nodes and are void from the ventricles. Moreover, we demonstrate that parasympathetic and sympathetic nerve axons develop synchronously and are intertwined throughout the ventricles. The cardiac neuronal networks are prone to causing pathology and fatal arrhythmias following an adult myocardial infarction. Interestingly, an infarction in the neonatal mouse results in robust heart regeneration with restored autonomic functions. In this study, we demonstrate that precise reinnervation occurs in the regenerating heart following injury, in stark contrast to the non-regenerating hearts. Remarkably, the regenerating myocardium reestablishes parasympathetic and sympathetic axon bundling, which we define in this study. Mechanistically, we demonstrate that this neuroplasticity is dependent on collateral artery formation, which precedes reinnervation during regeneration. These novel discoveries provide evidence that physiological reinnervation occurs uniquely during neonatal heart regeneration.

15. SUBJECT TERMS

cardiac nerves; cardiac regeneration; myocardial infarction; coronary vasculature; choline acetyltransferase; parasympathetic innervation; connexin 40

16. SECURITY CLASSIFICATION OF:			**17. LIMITATION OF ABSTRACT**	**18. NUMBER OF PAGES**	**19a. NAME OF RESPONSIBLE PERSON**
					USAMRDC
a. REPORT	**b. ABSTRACT**	**c. THIS PAGE**			**19b. TELEPHONE NUMBER** *(include area code)*
Unclassified	Unclassified	Unclassified	Unclassified	51	

TABLE OF CONTENTS

INTRODUCTION:
Our goal is to establish the role of cardiac nerves after injury to understand and harness their therapeutic potential in many cardiac pathologies. Gaining insights into the patterns of cardiac innervation and nerve density is necessary to promote physiological reinnervation in many cardiomyopathies. Our current understanding of cardiac nerve patterns following injury is largely based on histological analysis, where fixed tissues are labeled with different markers for visualization of neurons. This approach is very limited and cannot identify nerve patterns and clonal expansion of individual cells in a three-dimensional context and cannot reconstruct the complex patterns of nerves and networks with other cell types. In this research project, we employ comprehensive lineage tracing and clonal analysis of cardiac nerves while visualizing them in a three-dimensional (3D) manner together with coronary vessels to dissect the cardiac autonomic nervous system to understand the role of nerves during heart disease and regeneration.

KEYWORDS:
cardiac nerves; cardiac regeneration; myocardial infarction; coronary vasculature; choline acetyltransferase; parasympathetic innervation; connexin 40

ACCOMPLISHMENTS:
Major Goals:

Specific Aim 1: Elucidate the innervation patterns and clonal dynamics of cardiac nerves following adult cardiac injury.	**Timeline**	**Site 1**	**Site 2***	**Completion date or percentage of completion**
Major Task 1: Constructing the spatiotemporal map of cardiac nerve patterning during pathological innervation following adult cardiac injury.	Months			
Subtask 1: ACURO Approval	2-3	Dr. Mahmoud	Dr. Ardehali	07/2022
Subtask 2: Genetic labeling of cardiac nerves using the pan neuronal Cre mouse line (*Actl6b^{Cre})* in combination with the Rosa26-Tdtomato (*Rosa26^{tdT})* reporter mouse line. (Mice Number: 250)	1-4	Dr. Mahmoud		12/2022
Subtask 3: Performing adult myocardial infarction surgeries in transgenic mice.	3-6	Dr. Mahmoud		01/2023
Subtask 4: Measuring echocardiographic parameters and performing immunohistochemical analyses and whole mount imaging to evaluate cardiac nerve patterns.	6-10	Dr. Mahmoud		03/2023
Milestone(s) Achieved: Defining cardiac innervation patterns following adult myocardial infarction by adult surgeries, immunostaining, and whole mount 3D imaging. IACUC Approval in place.	1-10			Completed
Major Task 2: Clonal analysis of cardiac nerve remodeling following injury				

Subtask 1: Nerve cell clonal analysis using the cholinergic *ChAt*^{CreER} and the sympathetic *TH*^{CreER} in combination with the Rainbow mouse (*R26*$^{VT2/GK}$) following injection of limiting amounts of tamoxifen at multiple timepoints following injury. (Mice Number: 30)	3-6		Dr. Ardehali	12/2022
Subtask 2: Identifying cholinergic and sympathetic nerve cell clone expansion together with EdU staining to define nerve cell clonal dynamics.	7-9		Dr. Ardehali	02/2023
Subtask 3: 3D mapping of nerve cell clones over a time course of 4 weeks following adult cardiac injury. (Mice Number: 30)	8-12		Dr. Ardehali	04/2023
Milestone(s) Achieved: Clonal nerve cell expansion of individual cardiac nerves in adult mice following injury, which will define the dynamics of cardiac innervation during cardiomyopathy. IACUC Approval in place.	3-12			Achieved, and first manuscript submitted.
Specific Aim 2: Define the molecular signature of cardiac nerves during pathological reinnervation following injury.				
Major Task 3: Single cell gene expression analysis of cardiac nerves following adult cardiac injury				
Subtask 1: Performing adult cardiac injury in adult mice. (Mice Number: 16 mice)	12-16	Dr. Mahmoud		N/A
Subtask 2: Preparing cDNA libraries of isolated single cell cardiac nerves. Gene expression analysis and pseudotime analysis of single cell cardiac nerves following adult cardiac injury.	12-24	Dr. Mahmoud		N/A
Subtask 3: Prepare manuscript for publication. Attend conferences (American Heart Association Basic Science Cardiovascular) to present findings.	18-24	Dr. Mahmoud	Dr. Ardehali	First manuscript submitted
Milestone(s) Achieved: Single cell RNA sequencing and gene expression analysis to identify key target genes that regulate cardiac innervation following adult cardiac injury. IACUC Approval in place.	12-24			

What was accomplished under these goals?

Major activities and Specific Objectives: We completed all initial goals for this aim, with modifications detailed. We used genetic models, whole-mount imaging, and three-dimensional (3D) modeling tools to accurately define cardiac nerve architecture and neurovascular association during development. These techniques allowed us to generate and analyze the first 3D neurovascular map of the mature, intact murine heart ventricles (**Figures 1 & 3**). We use this system to further explore neurovascular development (**Figure 2**) and distribution of the parasympathetic and sympathetic nerve subpopulations (**Figure 1**). Furthermore, we reconstructed nerve patterning with high-spatial accuracy by employing comprehensive lineage tracing, whole-mount immunostaining, confocal microscopy, and 3D reconstruction during heart regeneration and disease. To distinguish between nerve remodeling in regenerating and non-regenerating hearts, we performed MI surgery at the regenerative (P1) and non-regenerative (P7) timepoints and collected hearts at 21 days post-MI. Our results demonstrate that nerve remodeling that follows neonatal and adult heart injury vary widely. The diseased, non-regenerative heart shows hallmarks of nerve pathology including denervation, hyperinnervation, and a novel phenotype of disassociation between the parasympathetic and sympathetic nerves (**Figure 4**)

Uniquely, the regenerating neonatal heart is precisely reinnervated, where the parasympathetic and sympathetic nerves are closely bundled throughout the regenerated myocardium (**Figure 4C**). To determine whether reinnervated axons associate with collateral arteries in the regenerating myocardium, we compare nerve-artery association in the regenerated and diseased heart. Our results demonstrate extensive reinnervation of the regenerated myocardium (**Figure 5D**). Excitingly, the nerves show reestablishment of nerve-artery connection with the collateral arteries, suggesting targeted innervation takes place. To determine whether reinnervation is dependent on collateral artery formation, we impaired collateral artery formation using the Cx40CreER;Cxcr4$^{fl/fl}$ mouse [37] (**Figure 6**), where deletion of Cxcr4 using the Cx40CreER mice impairs collateral artery formation during neonatal heart regeneration. Strikingly, the infarcted area was denervated in Cx40CreER;Cxcr4$^{fl/fl}$ hearts, in contrast to the regenerated and reinnervated wild type controls (**Figure 6B-C**), demonstrating that reinnervation is dependent on collateral artery formation.

Significant results: Remarkably, our approach reveals for the first time that parasympathetic nerves extensively innervate the cardiac ventricles. Furthermore, we provide evidence that parasympathetic and sympathetic nerves develop synchronously and are intertwined throughout the ventricles. Our results demonstrate that cardiac nerves sequentially associate with coronary veins and arteries during development. Our results demonstrate a unique physiological nerve remodeling during neonatal heart regeneration, where sympathetic and parasympathetic nerve bundles precisely reinnervate the collateral arteries in the regenerating myocardium, a process distinct from the pathological remodeling of the non-regenerating heart. Mechanistically, we use genetic inhibition of collateral arteries to demonstrate that physiological reinnervation during regeneration is dependent on collateral artery formation.

Unmet goals and problems encountered: For neurovascular association, we previously planned to use vascular markers for large-diameter vessels (αSMA) and a pan vascular marker (lectin). These markers were not compatible with whole-mount imaging (which requires markers that are highly expressed and high-affinity antibodies), so we shifted towards using the arterial cell reporter line Cx40^{CreER};Rosa26^{tdT}, combined with immunostaining for a different pan-vascular marker (Endomucin, EMCN) along with the pan-neuronal marker (Beta-Tubullin III, Tuj1).

What opportunities for training and professional development has the project provided?
Nothing to Report

How were the results disseminated to communities of interest?
The current results are now in a submitted manuscript for publication, which is also available as a preprint. Salamon, R.J., Halbe, P., Kasberg, W., Bae, J., Audhya, A., Mahmoud, A.I.*. Defining cardiac nerve architecture during development, disease, and regeneration. bioRxiv, doi: 10.1101/2022.12.31.522405 (*corresponding author).

What do you plan to do during the next reporting period to accomplish the goals?
We plan to perform RNA sequencing to determine the factors that regulates the physiological reinnervation in the regenerating heart, and whether these factors can restore physiological innervation patterns in the non-regenerating hearts. This will define the mechanisms that control cardiac innervation during disease and regeneration.

IMPACT:
What was the impact on the development of the principal discipline(s) of the project?
Our research highlights seminal findings about cardiac nerve architecture and neuroplasticity, which has direct clinical implications. In this work, we model the intact, mammalian cardiac nervous system and neurovascular network in high-resolution using lineage tracing, tissue clearing, whole-mount imaging, and 3D modeling. Excitingly, our results identify extensive parasympathetic innervation in the cardiac ventricles, challenging the clinical misconception that parasympathetic nerves only innervate the cardiac nodes and are void from the ventricles. Moreover, we demonstrate that parasympathetic and sympathetic nerve axons develop

synchronously and are intertwined throughout the ventricles. We further define nerve architecture by quantifying nerve distribution, branching level, and density in the embryonic and postnatal heart.

The cardiac neuronal networks are prone to causing pathology and fatal arrhythmias following an adult myocardial infarction. Interestingly, an infarction in the neonatal mouse results in robust heart regeneration with restored autonomic functions. In this study, we demonstrate that precise reinnervation occurs in the regenerating heart following injury, in stark contrast to the non-regenerating hearts. Remarkably, the regenerating myocardium reestablishes parasympathetic and sympathetic axon bundling, which we define in this study. Mechanistically, we demonstrate that this neuroplasticity is dependent on collateral artery formation, which precedes reinnervation during regeneration. Together, these novel discoveries provide evidence that the process of physiological reinnervation occurs uniquely during neonatal heart regeneration.

What was the impact on other disciplines?
Nothing to Report

What was the impact on technology transfer?
Nothing to Report

What was the impact on society beyond science and technology?
Our research has uncovered an unappreciated role for cardiac nerves during development, disease, and regeneration. Some novel insights such as the identification of extensive innervation of the cardiac ventricles will lead to new public knowledge that is more advanced than current medical textbooks.

CHANGES/PROBLEMS:
Changes in approach and reasons for change: Nothing to Report
Actual or anticipated problems or delays and actions or plans to resolve them: Nothing to Report
Changes that had a significant impact on expenditures: Nothing to Report
Significant changes in use or care of human subjects, vertebrate animals, biohazards, and/or select agents:
Nothing to Report

PRODUCTS:
Publications, conference papers, and presentations
Journal publications.
Salamon, R.J., Halbe, P., Kasberg, W., Bae, J., Audhya, A., Mahmoud, A.I.*. Defining cardiac nerve architecture during development, disease, and regeneration. bioRxiv, doi: 10.1101/2022.12.31.522405 (*corresponding author).

Books or other non-periodical, one-time publications.
Nothing to Report

Other publications, conference papers, and presentations.
Website(s) or other Internet site(s)
Nothing to Report
Technologies or techniques
Nothing to Report
Inventions, patent applications, and/or licenses
Nothing to Report
Other Products
Nothing to Report

PARTICIPANTS & OTHER COLLABORATING ORGANIZATIONS:

What individuals have worked on the project?

Name:	Ahmed Mahmoud
Project Role:	PD/PI
Researcher Identifier (e.g. ORCID ID):	0000-0003-1528-7393
Nearest person month worked:	2
Contribution to Project:	Dr. Mahmoud has performed work on the tasks specified in the table found in the major goals section of this report.
Funding Support:	This award

Name:	Reza Ardehali
Project Role:	Subaward PD/PI
Researcher Identifier (e.g. ORCID ID):	0000-0003-1318-4016
Nearest person month worked:	0.12
Contribution to Project:	Dr. Ardehali has performed work on the tasks specified in the table found in the major goals section of this report.
Funding Support:	This award

Name:	Rebecca Salamon
Project Role:	Research Assistant
Researcher Identifier (e.g. ORCID ID):	0000-0001-7934-1868
Nearest person month worked:	1
Contribution to Project:	Ms. Rebecca has performed the mapping of cardiac nerves during disease and regeneration.
Funding Support:	This award

Name:	Arash Pezhouman
Project Role:	Project Scientist
Researcher Identifier (e.g. ORCID ID):	0000-0001-9106-7136

Nearest person month worked:	1
Contribution to Project:	Dr. Pezhouman is a project scientist in Dr. Ardehali's lab and contributed work towards Dr. Ardehali's tasks.
Funding Support:	This award

Has there been a change in the active other support of the PD/PI(s) or senior/key personnel since the last reporting period?

Name of Individual: Mahmoud, Ahmed I

New

Title: Metabolic Reprogramming of the Adult heart to a Regenerative State

Major Goals: The goals of this project are to identify the mechanisms of succinate dehydrogenase regulation of adult heart regeneration.

Specific Aims: 1) Elucidate the metabolic and cellular mechanisms underlying post-MI regeneration following SDH inhibition; 2) Define the molecular mechanisms by which SDH inhibition promotes post-MI regeneration; 3) Determine the role of SDH inhibition by malonate on regenerative potential following myocardial infarction in a porcine model.

Project Number: 1R01HL166256-01

Name of PD/PI: Mahmoud, Ahmed

Source of Support: NHLBI, DHHS, PHS, National Institutes Of Health

Source of Support Address:

NIH/NHLBI Information center
P.O Box 30105
Bethesda, MD 20824-0105

Contracting/Grants Officer: Olga A. Tjurmina

Project/Proposal Start and End Date: (MM/YYYY): 03/2023 – 02/2027

Total Award Amount (including Indirect Costs):

Person Months (Calendar/Academic/Summer) per budget period.

Year (YYYY)	Person Months (##.##)
1. 2024	4.2 calendar
2. 2025	4.2 calendar
3. 2026	4.2 calendar
4. 2027	4.2 calendar

Newly Ended

Title: Nerve-Guidance of Post-Ischemic Heart Regeneration

Major Goals: The goal of this career development award is to identify the role of cholinergic nerve modulation of cardiomyocyte proliferation and inflammation during heart regeneration. **Specific Aims:** Aim 1. To test the hypothesis that cholinergic nerve regulation of heart regeneration is mediated through the cardiac M2 receptor. Aim 2. To dissect the mechanisms underlying Neuregulin 1 (NRG1) generation during neonatal mammalian heart regeneration. Aim 3. To test the hypothesis that cholinergic nerves regulate the inflammatory response during heart regeneration via nicotinic acetylcholine receptor signaling.

Project Number: 19CDA34660169

Name of PD/PI: Mahmoud, Ahmed

Source of Support: American Heart Association

Source of Support Address: American Heart Association
7272 Greenville Ave
Dallas, TX 75231

Contracting/Grants Officer: Cierra Vaughn-Smith

Project/Proposal Start and End Date: (MM/YYYY): 04/2019 – 03/2022
Total Award Amount (including Indirect Costs):
Person Months (Calendar/Academic/Summer) per budget period.

Year (YYYY)	Person Months (##.##)
1. 2020	4.8 calendar
2. 2021	4.8 calendar

Overlap: None

Title: Mapping Cardiac Innervation During Development, Disease, and Regeneration
Major Goals: The goal of this predoctoral award is to define cardiac innervation patterns during cardiac development and neonatal heart regeneration.
Specific Aims: The specific aim is to map nerve reinnervation in relevance to the coronary vasculature following injury.
Project Number: 829586
Name of PD/PI: Salamon, Rebecca; Mahmoud, Sponsor
Source of Support: American Heart Association
Source of Support Address: American Heart Association
7272 Greenville Ave
Dallas, TX 75231
Contracting/Grants Officer: Cierra Vaughn-Smith
Project/Proposal Start and End Date: (MM/YYYY): 04/2021 – 03/2023
Total Award Amount (including Indirect Costs):
Person Months (Calendar/Academic/Summer) per budget period.

Year (YYYY)	Person Months (##.##)
1. 2022	0 calendar
2. 2023	0 calendar

Overlap: This predoctoral award overlapped with Aim 1 of the proposal, as this student was contributing to the project and the predoctoral award was covering the student's salary.

Name of Individual: Ardehali, Reza
Newly Ended
Title: Vascular Biology Training Grant
Time Commitments: 1.2 calendar
Supporting Agency: NIH/NHLBI 5 T32 HL 069766
PI: Reza ARDEHALI
Address: Building 31, 31 Center Drive, Bethesda, MD 20892
Contracting/Grants Officer: Lidman, Karin Fredriksson
Performance Period: 05/01/18-03/31/23
Level of funding:
Project Goals: This grant aims to provide support to train graduate students and postdoctoral fellows in vascular biology.
Specific Aims: No specific aims
Overlap: None

Year (YYYY)	Person Months (##.##)
2018	1.2
2019	1.2

2020	1.2
2021	1.2
2022	1.2
2023	1.2

Title: The Role of Pericytes in Scar Formation Following Stroke and Myocardial Infarction.
Time Commitments: 1.8 calendar
Supporting Agency: NIH/NINDS 50R01 NS 112256
PI: Stanley Thomas CARMICHAEL
Address: NIH Neurological Institute, P.O. Box 5801, Bethesda, MD 20824
Contracting/Grants Officer: Bosetti, Francesca, Ph.D.
Performance Period: 03/01/20-01/16/23
Level of funding:
Project Goals: This grant investigates the role of perivascular cells in fibrosis after myocardial infarction and stroke.
Specific Aims: Aim 1: to use novel lineage-tracing techniques to investigate proliferation and migration of pericytes to the site of injury and examine their participation in scar formation. Aim 2: to perform single-cell gene expression profiling of brain and heart pericytes before and after injury to map the transcriptional changes of pericytes as they become pro-fibrotic. Aim 3: to determine the molecular mechanisms that regulate pericyte activation by performing gain and loss of function using in vitro and in vivo models.
Overlap: None

Year (YYYY)	Person Months (##.##)
2020	1.8
2021	1.8
2022	1.8
2023	1.8

Title: Sex Differences in Cardiac Fibrosis and Hypertrophy
Time Commitments: 0.6 calendar months
Supporting Agency: CDMRP W81XWH-21-1-0115
PI: Reza ARDEHALI
Address: 1077 Patchell Street, Bldg 1054, Fort Detrick, MD 21702-5024
Contracting/Grants Officer: Rahul G. Thakar, Ph.D.
Performance Period: 01/01/21-12/31/22
Level of funding:
Project Goals: This grant aims to investigate how gender difference impacts development and progression of scar and wall thinking in the injured heart.
Specific Aims: Aim1. To identify genes and pathways associated with sex differences in cardiac fibrosis in mice exposed to isoproterenol infusion. Aim 2. To identify genes and pathways associated with sex differences in hypertrophy in mice exposed to isoproterenol infusion.
Overlap: None

Year (YYYY)	Person Months (##.##)
2021	.6
2022	.6

Title: The Role of Neural Crest Progenitors in the Development of Ventricular Outflow Tract Defect
Time Commitments: 0.6 calendar months
Supporting Agency: CDMRP W81XWH-21-1-0150
PI: Jua-Nian CHEN

Address: 1077 Patchell Street, Bldg 1054, Fort Detrick, MD 21702-5024
Contracting/Grants Officer: Rahul G. Thakar, Ph.D.
Performance Period: 01/01/21-12/31/22
Level of funding:
Project Goals: This grant aims to investigate how the neural crest progenitors contribute to the formation of the outflow tract in mice and fish.
Specific Aims: Aim1. Determine the neural crest contributions to the developing zebrafish heart. Aim 2. Determine the contribution of neural crest progenitors to cardiomyocytes during mouse cardiac development.
Overlap: None

Year (YYYY)	Person Months (##.##)
2021	.6
2022	.6

Title: Engineering Cardiomyocyte Function by Controlled Mitochondrial Transfer
Time Commitments: 0.6 calendar months
Supporting Agency: CDMRP W81XWH-21-1-0139
PI: Michael TEITELL
Address: 1077 Patchell Street, Bldg 1054, Fort Detrick, MD 21702-5024
Contracting/Grants Officer: Rahul G. Thakar, Ph.D.
Performance Period: 01/01/21-12/31/22
Level of funding:
Project Goals: This grant aims to explore mechanistic insight into intercellular mitochondria transfer and the retention of exogenous mtDNA in new host cardiomycoytes.
Specific Aims: Aim1. To generate CMs with specific mtDNA sequences. Aim 2. To quantify transferred mtDNA expansion in CMs. Aim 3. To identify chromatin and gene expression changes in mtDNA-recipient CMs.
Overlap: None

Year (YYYY)	Person Months (##.##)
2021	.6
2022	.6

What other organizations were involved as partners?
Organization Name: THE REGENTS OF THE UNIVERSITY OF CALIFORNIA - LOS ANGELES
Location of Organization: 11000 Kinross Ave, Ste 211
Los Angeles, CA 90095-1406
Partner's contribution to the project: Dr. Reza Ardehali contributed effort on Task 1, Subtask 1; Task 2, Subtasks 1, 2, and 3; and Task 3, Subtask 3.

Appendix A: Figures

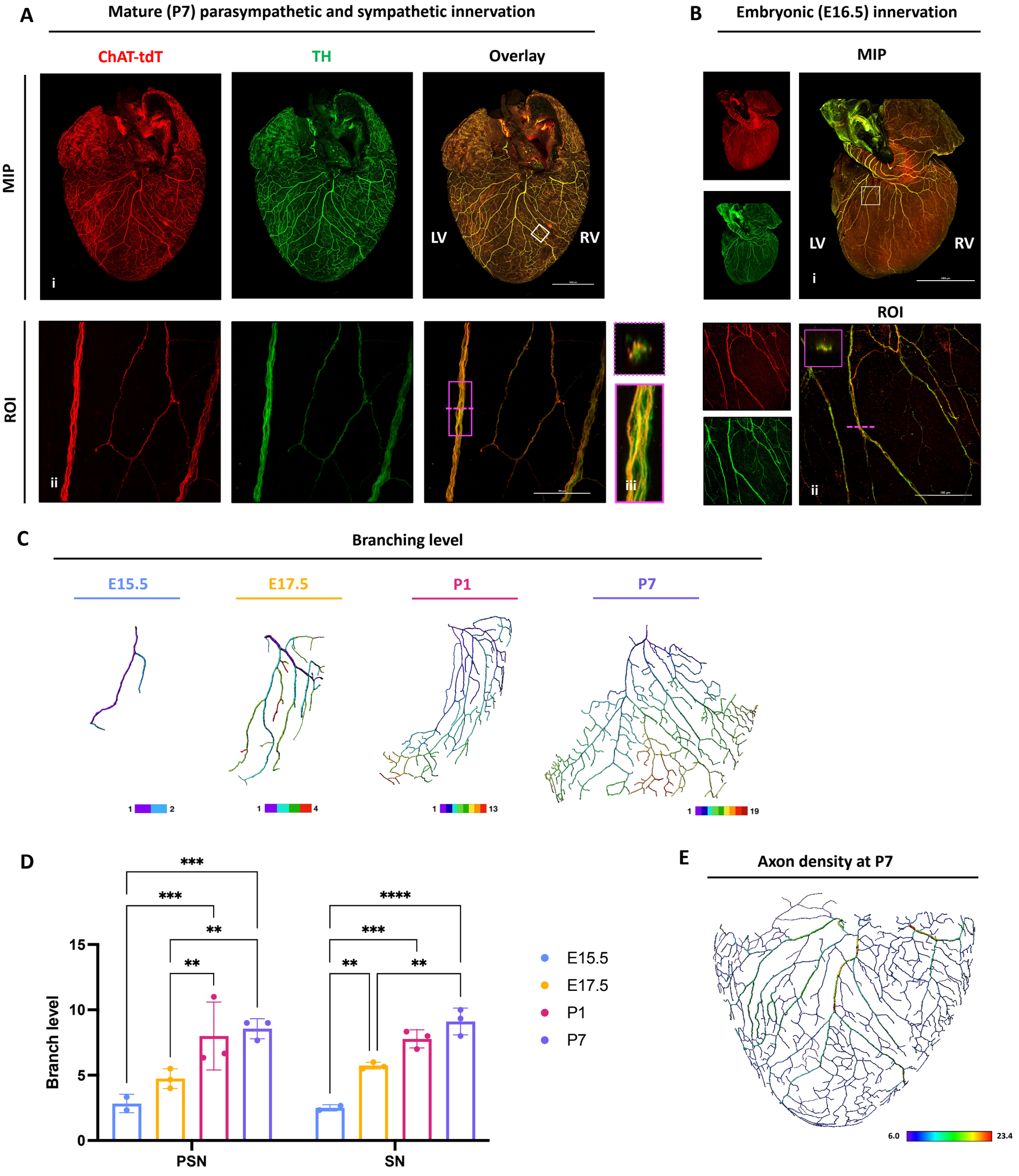

Figure 1. Parasympathetic and sympathetic nerves are bundled and synchronous in development. Parasympathetic reporter hearts (*ChATCre;Rosa26*^{tdTomato}) were immunostained for sympathetic nerves (tyrosine hydroxylase, TH), imaged with confocal microscopy, and reconstructed with Imaris. (A) The mature nerve patterning shows (A_i) close association between parasympathetic and sympathetic nerves, with (A_{ii}) large and small nerve fibers closely aligned and the (A_{iii}) large axons are bundled (n=5). (B) At E16.5, both parasympathetic and sympathetic axons extend together and are closely localized (n=6). (C-D) 3D modeling and analysis shows increased branching level during embryonic and postnatal development (n=3). (E) Density analysis of the P7 heart shows axon bundles of primary and secondary axons are at higher density than tertiary and higher branched axons.

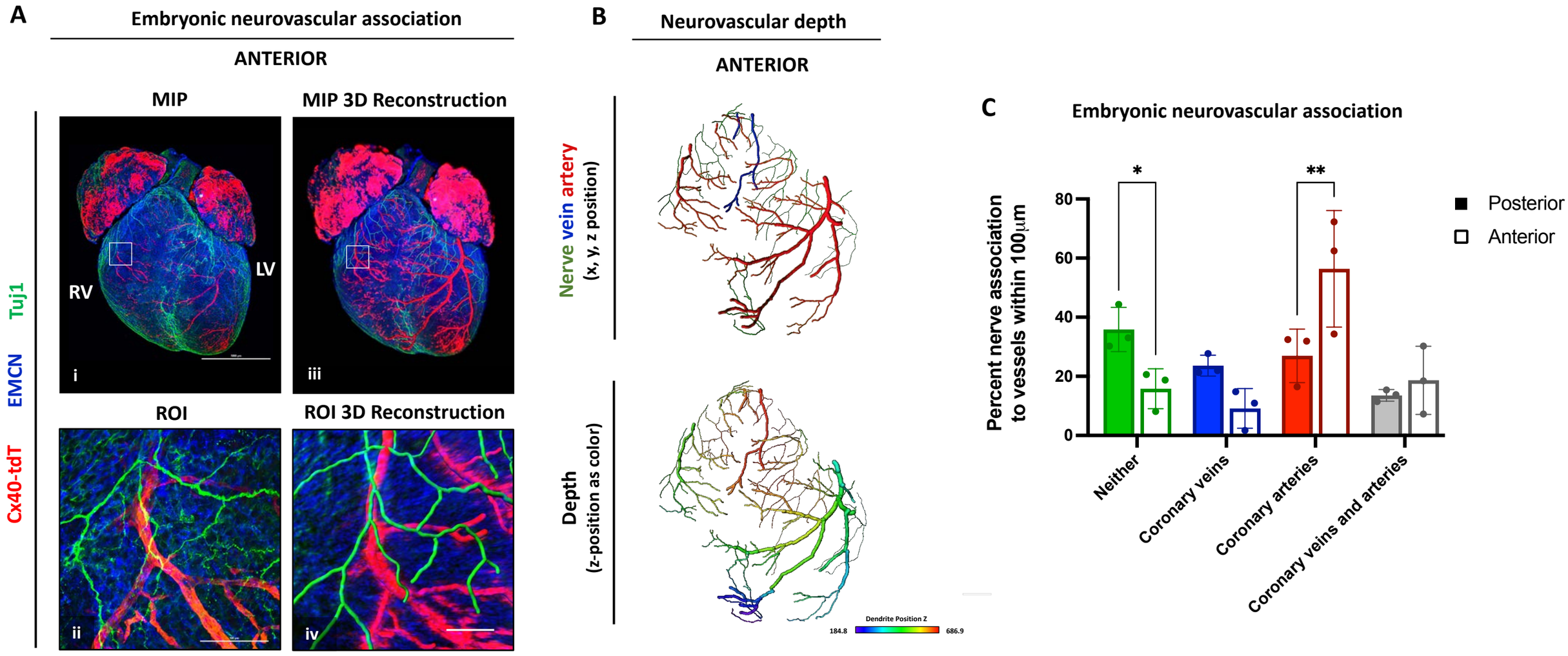

Figure 2. Neurovascular association shows cardiac axons align with the coronary arteries. Embryonic day 17.5 (E17.5) hearts of *Cx40CreER;Rosa26*^{tdTomato} mice were immunostained with Tuj1 and EMCN, followed by whole mount confocal imaging, and 3D reconstruction and modeling. The neurovascular patterning is shown as (A_i) a max intensity projection of the whole, anterior embryonic heart (A_{ii}) high magnification of ROIs (A_{iii}) 3D Imaris reconstruction of the whole embryonic heart, and (A_{iv}) reconstruction of ROIs (n=4). (B) Neurovascular depth analysis shows that the anterior nerves are at similar depths to the coronary arteries (n=3). (D) Quantification of percentage of nerves associated within 100um of coronary veins (blue), arteries (red) both veins and arteries (grey) or neither vessel type (green) are shown, with an increased nerve artery association in the anterior wall (n=3). Scale bars shown at 100um.

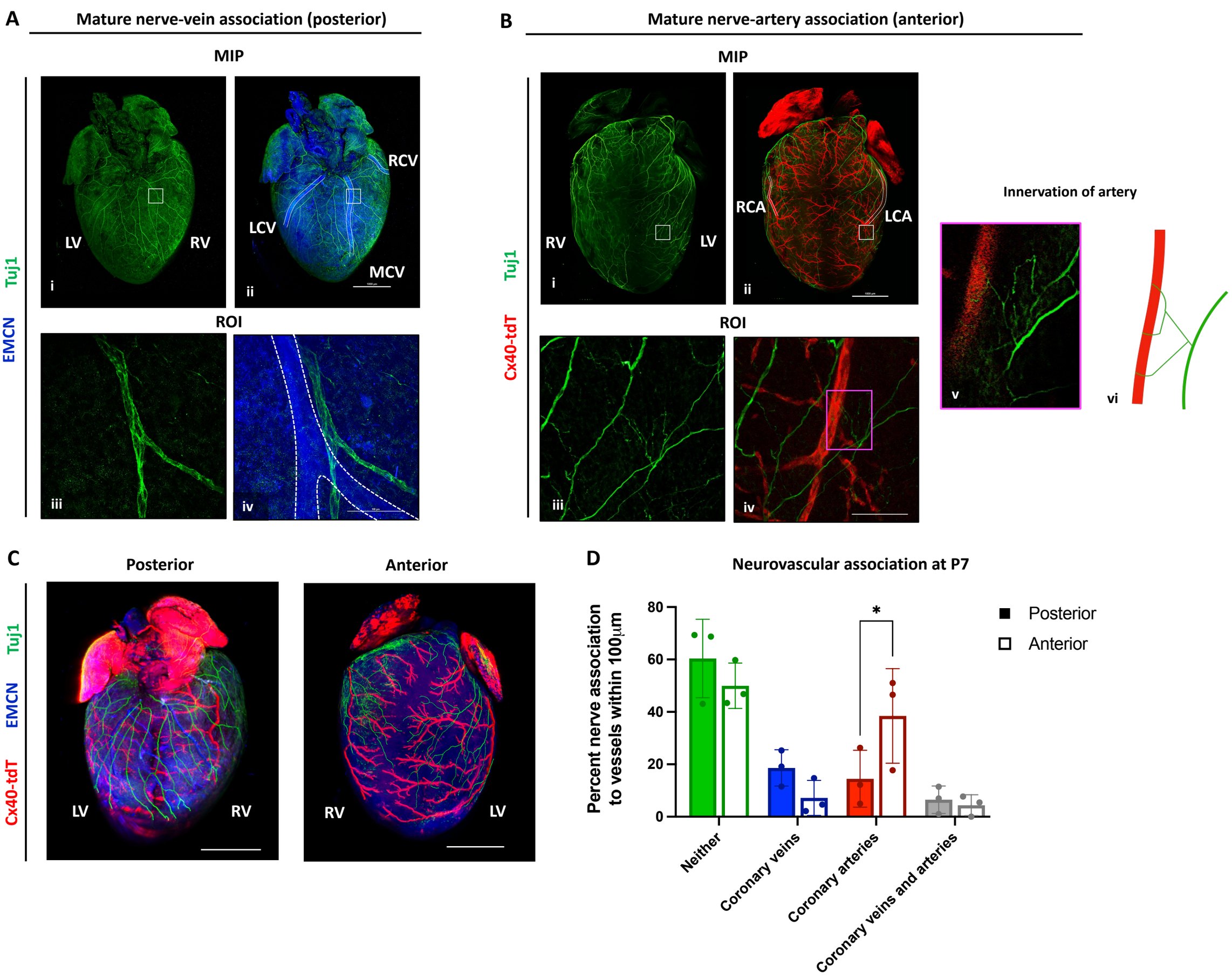

Figure 3. Mature 3D neurovascular architecture. P7 hearts of the *Cx40CreER;Rosa26^{tdTomato}* mice were immunostained with the pan-neuronal marker Tuj1 and the endothelial cell marker endomucin (EMCN), followed by CLARITY, whole mount confocal imaging, and 3D reconstruction. (A) The posterior wall distribution of the mature cardiac nerves is shown as a max intensity projection of patterning of (A_i) the posterior nerves alone and (A_{ii}) nerve-vein association. (A_{iii-iv}) The nerves align without innervating the major left, medial, or right coronary veins (LCV, MCV, RCV), shown with a representative 40x image of the region of interest (ROI) (n=4). (B) The anterior nerve architecture similarly is shown as the (B_i) anterior nerve patterning and (B_{ii}) nerve-artery association. (B_{iii-vi}) Nerves align and directly innervate the right and left coronary arteries (RCA, LCA), (B_{vi}) shown with a magnified z-plane of direct artery innervation (n=5). (C) Imaris 3D reconstruction highlights the neurovascular architecture of the posterior and anterior heart (n=3). (D) Quantification of percent of nerves associated within 100um of coronary veins (blue), arteries (red) both veins and arteries (grey) or neither vessel type (green) are shown, with an increased nerve artery association in the anterior wall (n=3). Scale bar is shown at 100um.

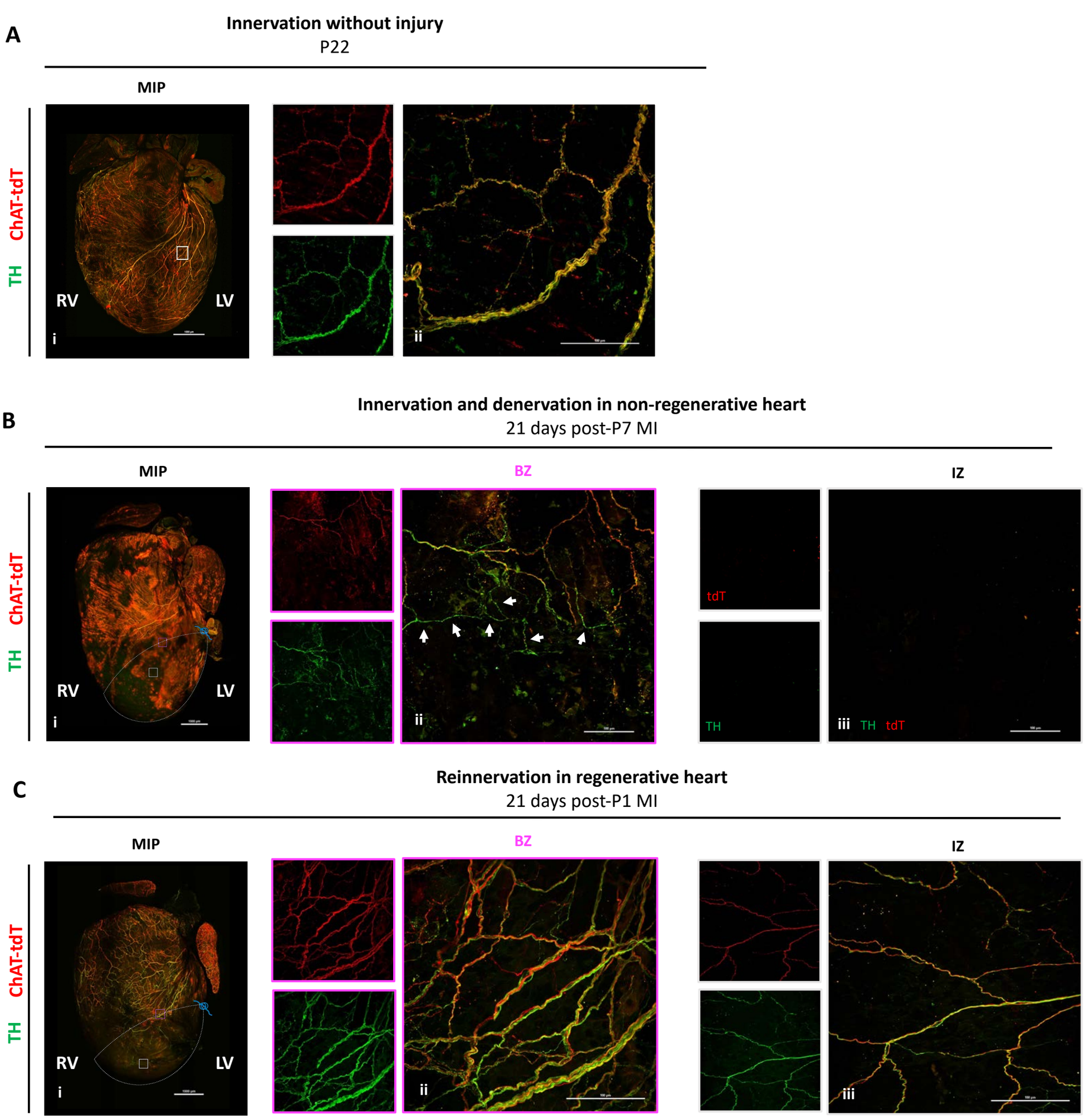

Figure 4. Parasympathetic and sympathetic nerves reinnervate the regenerated myocardium. Myocardial Infarction (MI) was performed on *ChATCre;Rosa26^{tdTomato}* mice at regenerative (P1) and non-regenerative (P7) timepoints. Hearts collected at 21 days post-MI, and immunostained for tyrosine hydroxylase (TH) and imaged with confocal microscopy. ($A_{i=ii}$) Uninjured hearts in adult (P22) mice show parasympathetic and sympathetic nerve entanglement in (A_i) whole mount and (A_{ii}) in the medial region of the myocardium (n=6). ($B_{i=iii}$) Non-regenerating hearts show pathological remodeling of the nerves. (B_{ii}) The border zone (BZ) shows reinnervation of sympathetic axons, independent of parasympathetic axons. (B_{iii}) The infarct zone (IZ) is denervated (n=6). ($C_{i=iii}$) The regenerated heart shows reestablished parasympathetic and sympathetic axon bundling. (C_{ii}) The BZ shows large nerve bundles of both nerve subtypes. (C_{iii}) The IZ shows reinnervation of parasympathetic and sympathetic axons (n=5). White dashed border indicates the IZ and the blue represents the suture site.

Figure 5

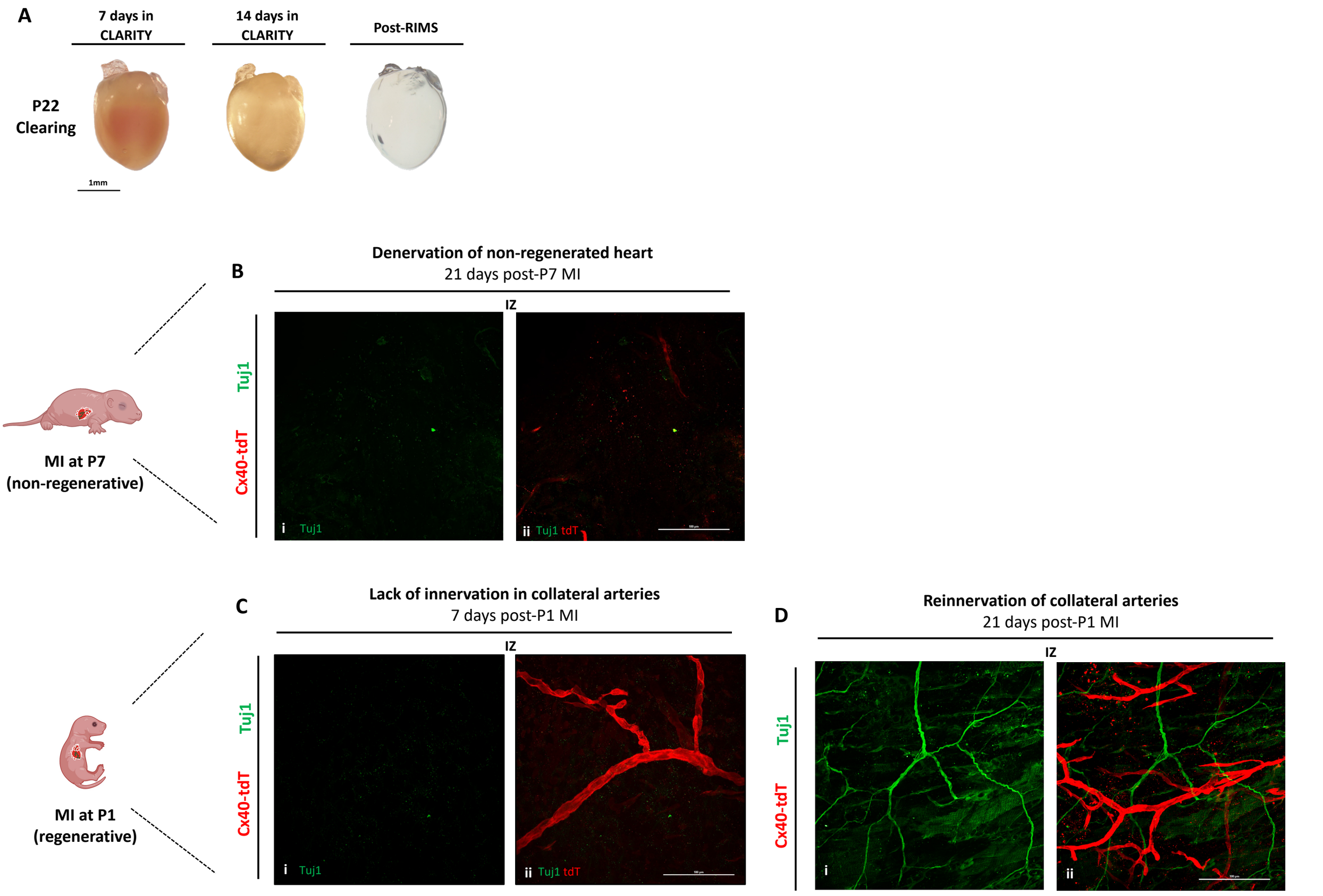

Figure 5. Nerve-artery association is reestablished in the regenerated heart. MI was performed in *Cx40CreER;Rosa26*^{tdTomato} in regenerative (P1) or non-regenerative (P7) mice. (A) Hearts were collected at 7- or 21-days post-MI and underwent tissue clearing and nerve immunostaining with Tuj1. ($B_{i\text{-}ii}$) Non-regenerative hearts at 21 days after P7 MI showed denervated and devascularization in the infarct zone (IZ), as expected due to the scar formation. ($C_{i\text{-}ii}$) Regenerative hearts at 7 days after P1 MI showed (B_i) the IZ is denervated, (B_{ii}) including the newly formed collateral arteries (n=6). ($C_{i\text{-}ii}$) By 21 days after P1 MI, (D_i) the regenerated tissue is reinnervated, (D_{ii}) with nerves showing artery association (n=4).

Figure 6

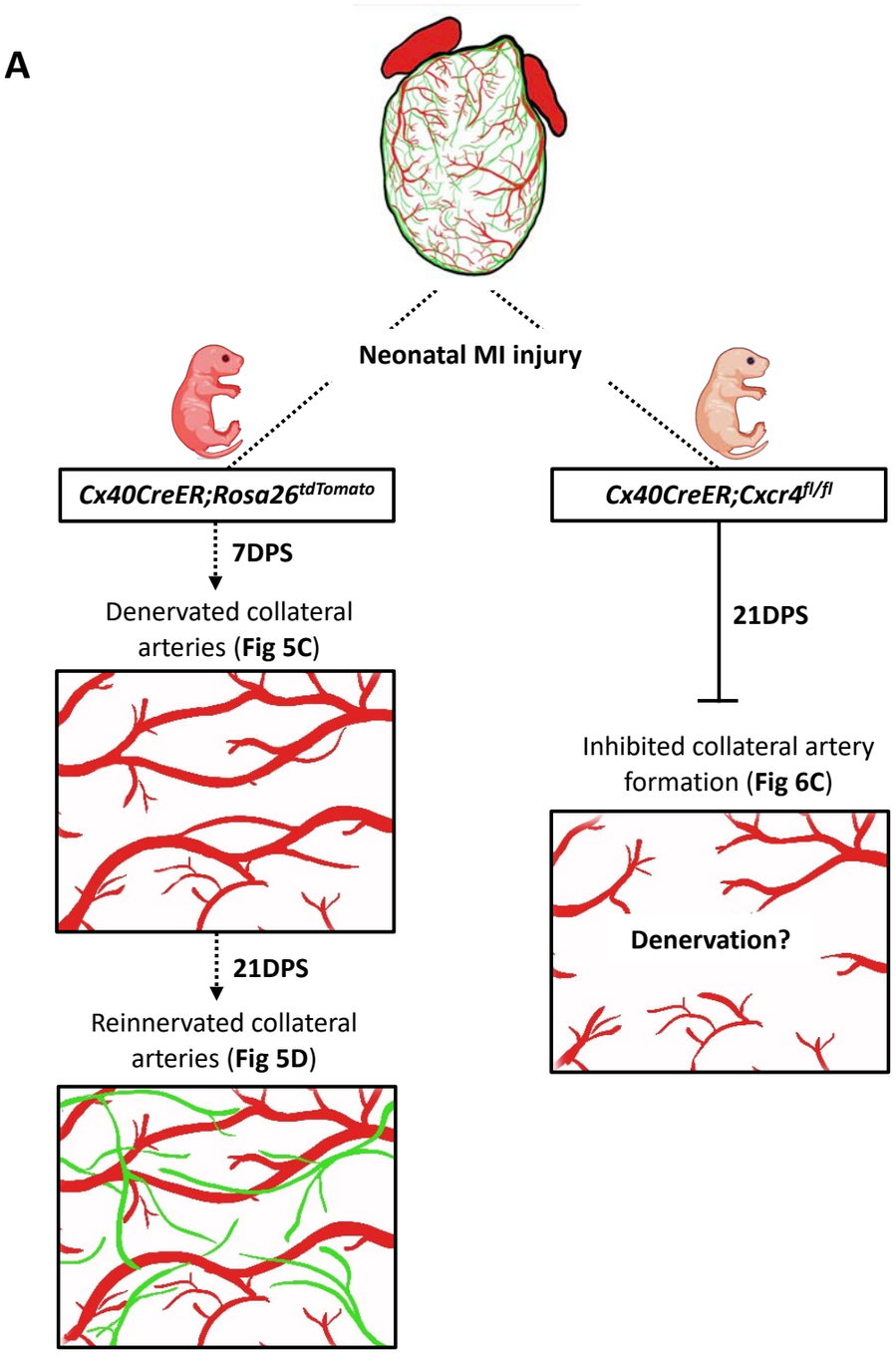

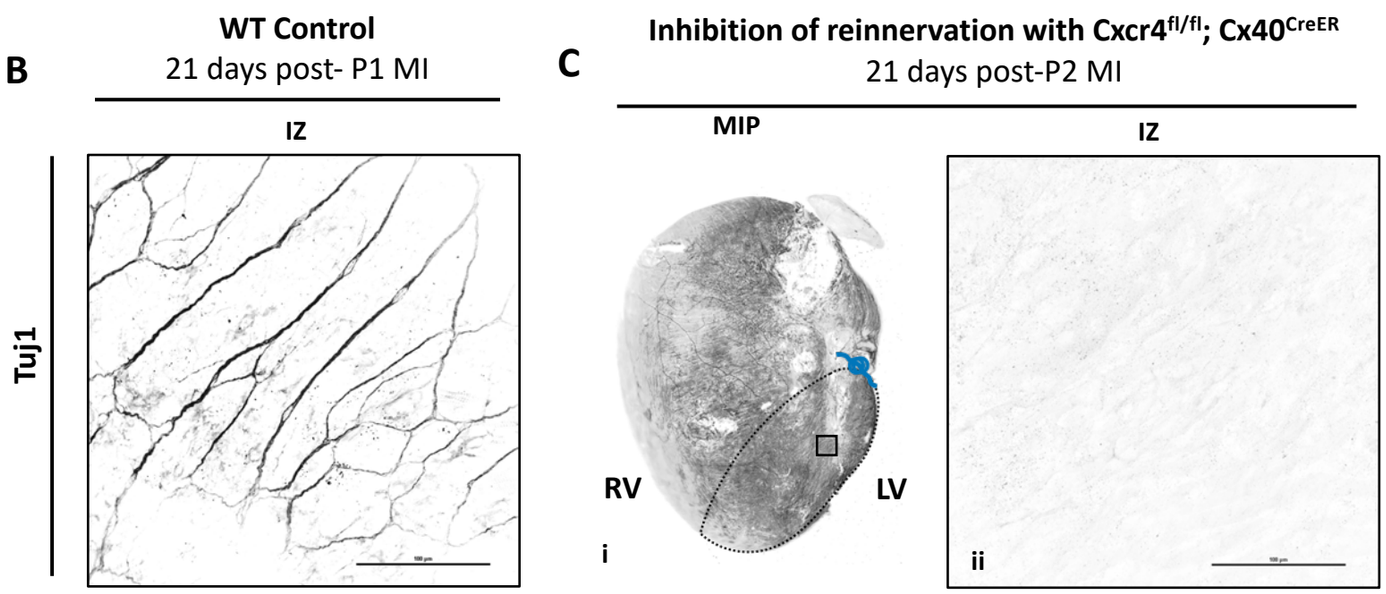

Figure 6. Reinnervation of the regenerating heart is dependent on collateral artery formation. MI was performed in *Cx40CreER;Rosa26^{tdTomato}* mice during the regenerative window (P2) and hearts were collected at 21-days post-MI. (A) We identify that the collateral arteries are reinnervated by 21-days post-MI. To determine whether reinnervation during regeneration is dependent on collateral artery formation, we used the *Cx40CreER;Cxcr4$^{fl/fl}$* mouse to inhibit migration of arterial cells post-MI. (C) At 21 days post-MI, Tuj1 immunostaining showed the IZ remained denervated in the *Cx40CreER;Cxcr4$^{fl/fl}$* mice (n=4), in comparison to (B) control regenerating hearts (n=4). Black dashed border indicates the IZ and the blue represents the suture site.

Appendix B: Journal Publication

Defining Cardiac Nerve Architecture During Development, Disease, and Regeneration

Rebecca J. Salamon[1], Poorva Halbe[1], William Kasberg[2], Jiyoung Bae[1,3], Anjon Audhya[2], Ahmed I. Mahmoud[1*]

[1]Department of Cell and Regenerative Biology, [2]Department of Biomolecular Chemistry, University of Wisconsin School of Medicine and Public Health, Madison, WI 53705, United States.

[3]Present address: Department of Nutritional Sciences, Oklahoma State University, Stillwater, OK 74078, United States.

*Corresponding author:
Ahmed I. Mahmoud, Ph.D.
University of Wisconsin-Madison School of Medicine and Public Health
1111 Highland Ave, Room 4557
Madison, WI 53705
Tel: +1 (608) 262-8682
Email: aimahmoud@wisc.edu

ABSTRACT

Cardiac nerves regulate neonatal mouse heart regeneration and are susceptible to pathological remodeling following adult injury. Understanding cardiac nerve remodeling can lead to new strategies to promote cardiac repair. Our current understanding of cardiac nerve architecture has been limited to two-dimensional analysis. Here, we use genetic models, whole-mount imaging, and three-dimensional modeling tools to define cardiac nerve architecture and neurovascular association during development, disease, and regeneration. Our results demonstrate that cardiac nerves sequentially associate with coronary veins and arteries during development. Remarkably, our results reveal that parasympathetic nerves densely innervate the ventricles. Furthermore, parasympathetic and sympathetic nerves develop synchronously and are intertwined throughout the ventricles. Importantly, the regenerating myocardium reestablishes physiological innervation, in stark contrast to the non-regenerating heart. Mechanistically, reinnervation during regeneration is dependent on collateral artery formation. Our results reveal how defining cardiac nerve remodeling during homeostasis, disease, and regeneration can identify new therapies for cardiac disease.

Keywords: cardiac nerves; cardiac regeneration; myocardial infarction; coronary vasculature; choline acetyltransferase; parasympathetic innervation; connexin 40

INTRODUCTION

The cardiac nervous system is a pillar of cardiac physiology, regulating conduction and contractility that is balanced by two opposing branches of the sympathetic and parasympathetic input [1]. Cardiac nerves localize to specialized nodes, the heart's pacemaker cells, where signals for contraction are propagated throughout the atria and into the ventricles [2, 3]. Recent studies led to new insights on the patterning and function of the intrinsic cardiac nervous system, which underscores the importance of dissecting the role of neurocardiology in cardiac health and disease [4, 5].

The influence of cardiac innervation expands beyond their well-known autonomic role in the heart. Specifically, sympathetic nerves have been demonstrated to extensively innervate the ventricles [6, 7]. These ventricular nerve networks mediate communication across a variety of cell types, including myocytes and blood vessels [8, 9]. Neural connections are established during late embryonic and early postnatal development by a co-maturation system [10, 11] where innervation patterning and maturation relies on signals from a variety of cardiac tissues [12, 13]. Interestingly, sympathetic nerves have been demonstrated to mediate the postnatal transition of cardiomyocytes from hyperplasia to hypertrophy [14] and cardiomyocyte size [15].

In contrast, parasympathetic innervation has been less studied for its interactions within the cardiac ventricles, due to the widely-held belief that parasympathetic nerves do not significantly contribute to ventricular innervation [16]. This misconception has recently been challenged by evidence of parasympathetic nerve function within the ventricles, including a high density of cells expressing muscarinic receptors [17, 18], protective functions against ventricular arrythmias [19], effects on

contractility influence [20], and distribution of parasympathetic nerve fibers [21-24]. Yet, the anatomy, distribution, and cell-cell interactions of ventricular parasympathetic innervation remains unclear.

Autonomic nerve remodeling and dysfunction contributes to the pathogenesis of cardiovascular disease [10, 25]. The heterogeneity of nerve remodeling, including regions of denervation and sympathetic hyperinnervation, has been demonstrated to contribute to ventricular arrhythmias and sudden cardiac death [25-29]. Interestingly, nerves play an important role in promoting repair and regeneration across a variety of organs and species [30]. Importantly, cholinergic nerve function regulates cardiomyocyte proliferation and regeneration of the neonatal mouse heart [31]. Remarkably, this regenerative response is accompanied with restoration of autonomic functions, suggesting physiological innervation of the regenerating mammalian heart [32]. However, how cardiac nerve patterning and distribution compares to the uninjured or diseased heart has not been explored.

The broadened role of the intrinsic cardiac nervous system in regulating heart development, homeostasis, and regeneration highlights the importance of defining the patterns of cardiac innervation as a necessary step to promote physiological reinnervation in many cardiomyopathies. Gaining insights into the patterns of cardiac innervation and nerve density during development is necessary to understand the normal circuitry of cardiac innervation. Our current understanding of cardiac nerve patterns is largely based on two-dimensional (2D) histological analysis, where fixed tissues are labeled with different markers for visualization of neurons. This approach is limited as it provides no information regarding their spatiotemporal distribution. Additionally, histological analysis cannot reveal information about the developmental distribution of neurons in the heart.

Thus, comprehensive lineage tracing of individual cardiac nerves while visualizing them in a three-dimensional (3D) manner is necessary to dissect the development, maturation, and lineage commitment of the cardiac autonomic nervous system.

Here we generate and analyze the first 3D neurovascular map of the mature, intact murine heart ventricles. We reconstruct nerve patterning with high-spatial accuracy by employing comprehensive lineage tracing, whole-mount immunostaining, confocal microscopy, and 3D reconstruction. We use this system to further explore neurovascular development and distribution of the sympathetic and parasympathetic subpopulations. We demonstrate that parasympathetic nerves extensively innervate the heart during development and in the postnatal heart together with sympathetic nerves, highlighting that parasympathetic nerves contribute significantly to ventricular innervation. Furthermore, we demonstrate physiological nerve remodeling during regeneration, which is distinct from pathological innervation of the non-regenerating heart. Mechanistically, we demonstrate that physiological reinnervation during regeneration is dependent on collateral artery formation. Together, our findings reconstruct cardiac nerve architecture and remodeling during development, disease, and regeneration.

METHODS

Mice

All animal experimental procedures were approved by the Institutional Animal Care and Use Committee of the University of Wisconsin-Madison. All experiments were performed on age and sex matched mice, with an equal ratio of male to female mice. Mouse lines used in this study are:

ChATCre (The Jackson Laboratory, Stock# 006410), *Rosa26*^{tdTomato} (The Jackson laboratory, Stock# 007905), *Cx40CreER* ([33], *Cxcr4*$^{fl/fl}$ (The Jackson laboratory, Stock# 008767).

Tamoxifen Administration

Tamoxifen was prepared at 100 mg/ml, dissolved in a 9:1 solution of corn oil to 100% ethanol, and incubated at 37ºC overnight with rotation. Solution was vortex as needed. Tamoxifen stock was kept at 4ºC for up to one month and incubated at 37ºC overnight before use. For *Cx40CreER* postnatal Cre induction, tamoxifen (1mg per pup) was administered by a subcutaneous (SubQ) injection directly to pup at P4 [34]. For *Cx40CreER* embryonic Cre induction, tamoxifen (0.1mg/g BW) was administered to the intraperitoneal (IP) cavity of the pregnant dam 24 hours before harvest.

Myocardial infarction surgery

Myocardial Infarction surgery (MI) was performed at P1 or P7, as described [35]. Pups were separated from dam and placed into a new cage with bedding. Pup was anesthetized on ice for 3 minutes. Working under a dissecting scope, a small incision was made in the skin, area under the skin was loosened, the 4th intercostal muscle was located, and incision was made, and the heart was gently guided out of the chest cavity with blunt forceps. The LAD was located at ligated with a 6-0 prolene suture by a surgeon's knot followed by a simple knot, and apical blanching was visualized. Heart was gently guided back into the chest cavity, ribs were sutured together, and skin was glued. Pup was placed into a heating pad until lively. Once surgery was complete, pups were rubbed with original bedding to transfer scent and placed back to dam. Hearts were collected at 7- or 21-days post-MI.

Tissue clearing of intact postnatal hearts

Our passive CLARITY technique was performed with minimal modifications [36] in hearts that required imaging of structures deep within the tissue (i.e. coronary arteries). Briefly, hearts were harvested, washed in PBS, and placed into a 2ml (embryonic to P7 hearts) or 4ml (P21+ hearts) glass vial with 4% PFA, incubating overnight at 4ºC with rotation. Following, hearts were washed with PBS for 30min at room temperature (RT), repeated three times, and placed into a polymerization solution (4% acrylamide and 0.5% VA-044) overnight at 4ºC. The next day, polymerization was activated with a 3-hour incubation at 37ºC. Hearts were again washed at RT in PBS for 1 hour, repeated three times. Hearts were placed into clearing solution (8.0% w/v SDS, 1.25% w/v Boric acid, 0.5% w/v 1-thiioglycerol dissolved in purified H2O, pH 8.5) and incubated at 37ºC, changing the solution every two days until tissue was fully cleared. Typically, P7 and P22 hearts were cleared for 5-7 or 14-16 days, respectively. In some tissues, a dark, green colored pigment persists even after clearing; regardless tissues were moved onto next steps, as it will be cleared out during washing. After clearing, tissues were washed in a conical tube with 10ml of PBS for 3 days, changing PBS solution 2-3 times daily.

Whole-mount immunohistochemistry

For uncleared tissues, hearts were harvested, blood removed, placed into a 2ml vial (for embryonic to P7 hearts) or 4ml vial (older than P7 hearts) and fixed for 1 hour in 4% PFA at 4ºC (for embryonic hearts) or RT (for postnatal hearts). Hearts were washed in PBS for 15 min, repeated 3 times.

Cleared and uncleared hearts underwent the same immunohistochemistry staining protocol described. Hearts were blocked in 20% blocking buffer (BB, matching serum from secondary host) made in PBS with 0.2% triton (PBST) for 1 hour at RT. Primary antibodies were diluted in 0.2% PSBT with 2% BB and at the following concentrations: rabbit RFP/tdTomato (Rockland, Cat# RL600-401-379) at [1:200], mouse Tuj1 (Sigma, Cat# T8453) at [1:200], rabbit Tuj1 at [1:500], sheep TH (Chemicon, Cat# AB1542) at [1:200], endomucin (Santa Cruz, Cat# SC65494) at [1:100]. Primary concentrations for hearts at P21 or older were doubled. Primary incubation was performed overnight at RT, then transferred to 4ºC for an additional overnight incubation. Following, hearts were washed with PBS for 30min at RT, repeated three times. Secondary antibodies were diluted in 0.2% PBST + BB at [1:250], using the following Alexa Fluor antibodies from Invitrogen: 594 anti-rabbit (Cat# A32740), 488 anti-mouse (Cat# A32723), 488 anti-sheep (Cat# A-11015), 405 anti-rat (A48261). Secondary incubation was performed for 3 hours at RT then moved to 4ºC overnight. When using a combination of mouse and rat primary antibodies, the staining was performed sequentially to limit cross-reaction of secondary antibodies [37].

Microscopy and 3D reconstruction

Confocal imaging was performed on a Nikon Upright FN1 microscope equipped with high sensitivity GaAsP detectors. Hearts were placed into a 3D-printed well, filled with water, and positioned for anatomical view. Whole heart images were taken using a 4x air objective (0.2 NA), with 5 um spacing between z-planes, and tiles stitched with Nikon pic-stitching function, and scale bars shown as 1 mm. Higher magnification images were taken using a 40x water immersion objective (0.8 NA), with 1 um steps between z-planes, and scale bars shown as 100 um. Imaris microscopy image analysis software in filaments mode was used to segment hearts generate

statistics. Representative images are shown as max intensity projections (MIP) and were edited using Adobe Lightroom and Photoshop for clarity. Since Endomucin (EMCN) stains veins and capillaries, EMCN signal in large-diameter veins was artificially highlighted in Photoshop. Confocal images were deconvolved using iterative classic maximum likelihood estimation in Huygens Profession before Imaris 3D reconstruction.

Statistical Analysis

Data generated via Imaris, with 2-3 replicates averaged per sample and 3 samples per group. Graphs generated in GraphPad Prism 9, with individual points representing the average per sample. Groups compared by an ordinary two-way ANOVA, with uncorrected Fisher's LSD, with a single pooled variance. Significance shown as n.s. ($P > 0.05$), * ($P \leq 0.05$). **($P \leq 0.01$), ***($P \leq 0.001$), **** ($P \leq 0.0001$).

RESULTS

Cardiac Nerves Sequentially Associate with Coronary Veins and Arteries During Development

The development of cardiac innervation throughout the ventricles of the embryonic heart is not completely defined. Our current understanding of cardiac nerve patterning of heart development is largely based on 2D analysis; however, this approach is insufficient to reconstruct the intricate nerve networks and cell-cell interactions. Specifically, although the coronary arteries are known to be innervated by sympathetic axons [13], the developmental timeline and patterning of artery innervation is not well defined. Here, we sought to elucidate the dynamics between nerve-vein and nerve-artery association during embryonic heart development.

The main, large-diameter veins of the embryonic heart primarily reside on the posterior wall [13], whereas the main coronary arteries are primarily located within the anterior wall [13, 38]. Therefore, we divided the architectural regions into posterior and anterior sides of the heart, including right and left ventricles (LV, RV) (**Figure 1**). Coronary arteries were visualized with lineage labeling using the inducible Connexin 40 Cre (*Cx40CreER*) and the *Rosa26*^{tdTomato} reporter mice (**Figure 1**). Neurovascular patterning was identified with additional markers for all nerves using beta tubulin III (Tuj1), and veins were labeled with endomucin (EMCN) (**Figures 1A-C**).

Sympathetic nerve axons innervate the heart as early as embryonic day (E) 13.5 via nerve growth factor (NGF) release by coronary veins, where sympathetic nerve axons become aligned with the veins of the posterior wall [13]. We confirmed that the axons aligned with posterior large-diameter veins from E15.5-E17.5 (**Figure 1A; Figure S1A-C**), verifying our use of EMCN to trace large-diameter veins. Since coronary arteries primarily reside on the anterior side of the ventricle at these developmental stages [38], we hypothesized that the anterior wall would have significant nerve-artery alignment. Supporting this, as early as E16.5, axons wrapped around from the posterior wall towards arteries in the anterior wall of the heart (**Figure 1B; Figure S1D-F**). By E17.5, the nerve patterning was associated with the anterior coronary arteries (**Figures 1B$_{i-iv}$**). These results demonstrate that nerve-artery association occurs within the anterior wall of the ventricle during late developmental stages.

We used 3D reconstruction to visualize and analyze the depth of innervation at E17.5 throughout multiple regions of the heart ventricles, where depth was defined as a function of z (**Figure 1C**).

The nerves showed similar depth to their closest vascular structure, with subepicardial nerves aligning closely with the coronary veins, and myocardial nerves aligning to the coronary arteries. Interestingly, the nerves in the base of the heart were more superficial than those in the periphery and apical regions; and this patterning was consistent on both posterior and anterior walls (**Figure 1C**). Depth analysis supports the regional correlation of posterior nerve-vein alignment and anterior nerve-artery association at E17.5 (**Figure 1D**) Our results demonstrate a programmed sequential and targeted innervation pattern with respect to vessel subtype, location, and depth throughout development.

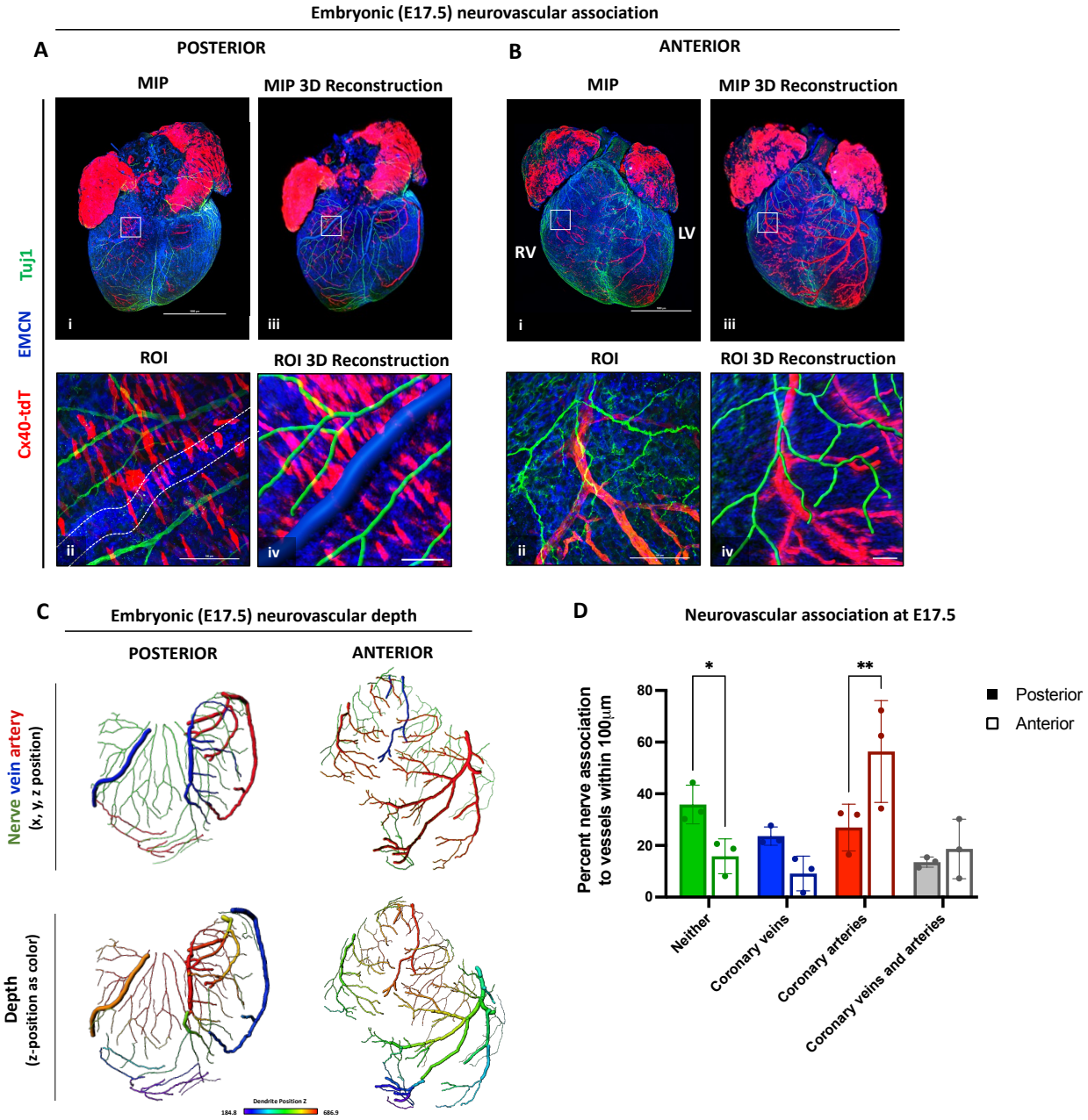

Figure 1. Neurovascular association shows cardiac axons align posteriorly with large veins and anteriorly with arteries. Embryonic day 17.5 (E17.5) hearts of *Cx40CreER;Rosa26*^{tdTomato} mice were immunostained with Tuj1 and EMCN, followed by whole mount confocal imaging, and 3D reconstruction and modeling. The neurovascular patterning is shown as (A-B$_i$) a max intensity projection of the whole embryonic heart (A-B$_{ii}$) high magnification of ROIs (A-B$_{iii}$) 3D Imaris reconstruction of the whole embryonic heart, and (A-B$_{iv}$) reconstruction of ROIs (n=4). (C)

Neurovascular depth analysis shows that the posterior and anterior nerves are at similar depths to the vascular structure closest in proximity (n=3). (D) Quantification of percentage of nerves associated within 100um of coronary veins (blue), arteries (red) both veins and arteries (grey) or neither vessel type (green) are shown, with an increased nerve artery association in the anterior wall (n=3). Scale bars shown at 100um.

Defining 3D Cardiac Nerve Architecture of the Postnatal Mouse Ventricle

Next, we sought to define typical nerve-vein and nerve-artery architecture in the postnatal heart. To rigorously define the 3D architecture of the postnatal heart ventricles, we considered that the spatial region of the heart is subject to natural biological variability of heart shape, size, and vascular patterning. To provide consistency between samples, we defined the architectural regions in two-fold. First, posterior and anterior sides of the heart were indicated, including right and left ventricles (LV, RV) as shown in Figure 1. Second, we used the well-defined vascular system, composed of the coronary veins and arteries, to demonstrate association of the nerves with these vessels. The coronary vessels are defined as the main right, medial and left coronary veins (RCV, MCV, LCV) and the right and left coronary arteries (RCA, LCA).

Hearts were collected at postnatal day (P) 7, a timepoint where co-maturation of the nerves and the myocardium takes place [10]. We utilized the *Cx40CreER;Rosa26*^{tdTomato} mice to label coronary arteries in addition to whole mount immunostaining for nerves with Tuj1 and veins with EMCN (**Figure 2**). Whole mount imaging of the posterior wall demonstrates nerve-vein alignment, where large nerve bundles were localized near the left, medial, and right coronary veins (**Figures 2A$_{i-iv}$**; LCV, RCV, MCV,), in agreement with previous reports [13]. Interestingly, the anterior wall

demonstrates that innervation is highly localized to the right and left coronary arteries (**Figures 2B$_{i-iv}$**; LCA, RCA). This close nerve-artery association allowed for axonal projections to directly innervate the arteries (**Figures 2B$_{v-vi}$**). Confocal images were reconstructed in 3D by Imaris and analyzed for neurovascular association (**Figures 2C-D**). This relationship between nerves, veins, and arteries is characterized and quantified to define the typical nerve patterning of the postnatal mouse heart. The anterior wall shows a significant increase in the percent of nerves associated with the coronary arteries, in comparison to the posterior wall distribution (**Figure 2D**). Our results construct the 3D cardiac nerve architecture within the cardiovascular network in the postnatal heart, revealing a distinct innervation pattern with coronary veins and arteries in the cardiac ventricles.

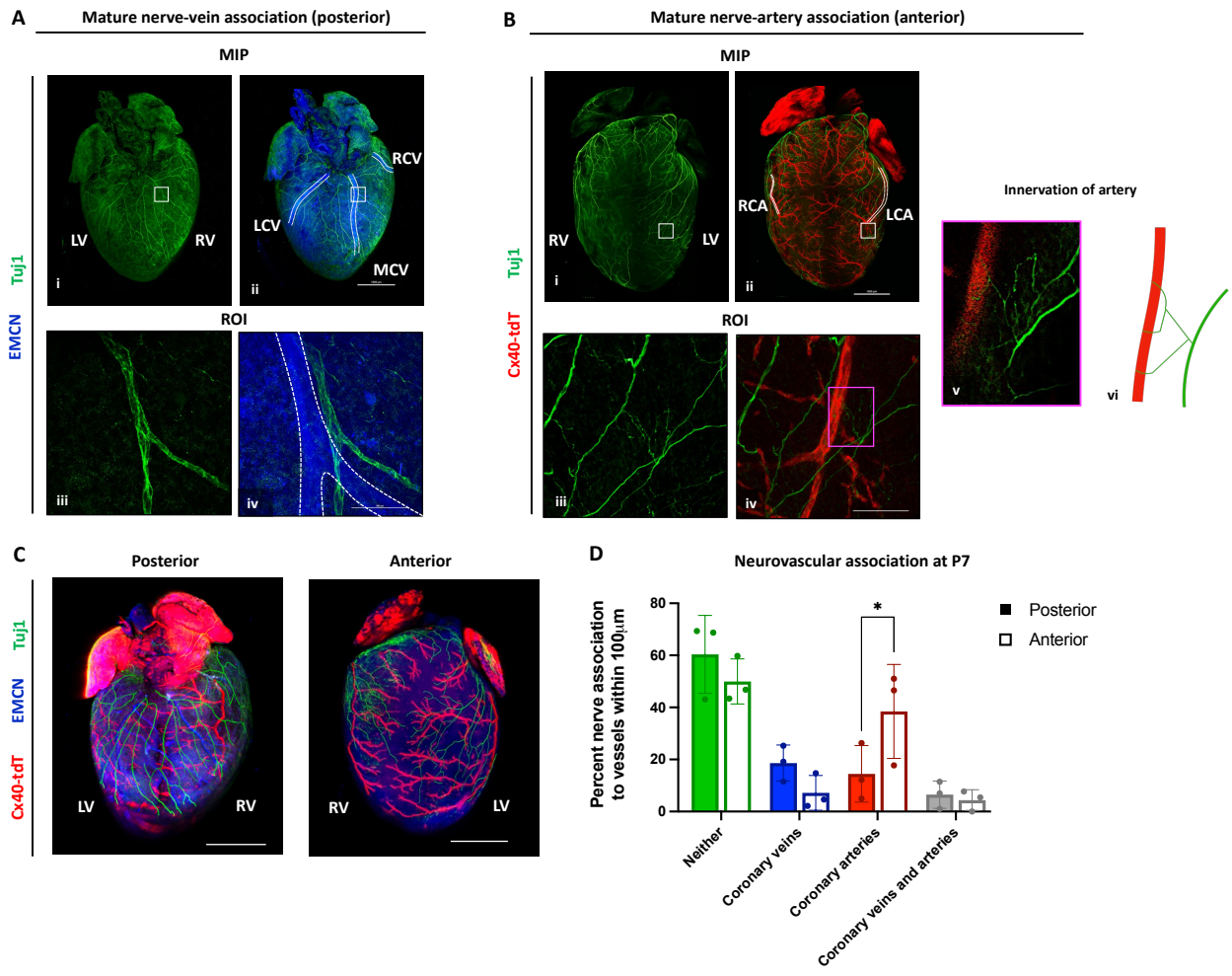

Figure 2. Mature 3D neurovascular architecture. P7 hearts of the *Cx40CreER;Rosa26*^{tdTomato} mice were immunostained with the pan-neuronal marker Tuj1 and the endothelial cell marker endomucin (EMCN), followed by CLARITY, whole mount confocal imaging, and 3D reconstruction. (A) The posterior wall distribution of the mature cardiac nerves is shown as a max intensity projection of patterning of (A_i) the posterior nerves alone and (A_{ii}) nerve-vein association. (A_{iii-iv}) The nerves align without innervating the major left, medial, or right coronary veins (LCV, MCV, RCV), shown with a representative 40x image of the region of interest (ROI) (n=4). (B) The anterior nerve architecture similarly is shown as the (B_i) anterior nerve patterning and (B_{ii}) nerve-artery association. (B_{iii-vi}) Nerves align and directly innervate the right and left coronary arteries (RCA, LCA), (B_{vi}) shown with a magnified z-plane of direct artery innervation (n=5). (C) Imaris 3D reconstruction highlights the neurovascular architecture of the posterior and anterior heart (n=3). (D) Quantification of percent of nerves associated within 100um of coronary veins (blue), arteries (red) both veins and arteries (grey) or neither vessel type (green) are shown, with an increased nerve artery association in the anterior wall (n=3). Scale bar is shown at 100um.

Parasympathetic and Sympathetic Nerves Develop Synchronously and are Closely Localized Throughout Postnatal Maturation

Recent evidence suggests that parasympathetic innervation and function has an underappreciated role in the cardiac ventricles. However, the patterning and distribution of the parasympathetic innervation has not been well defined. To define the parasympathetic nerve patterning with respect to sympathetic innervation in the intact heart, we used our 3D imaging and analysis pipeline with a parasympathetic reporter mouse line and immunostaining for the sympathetic nerves. For parasympathetic nerve lineage labeling, we used the *ChATCre* knockin mouse with the

Rosa26^{tdTomato} reporter (*ChATCre;Rosa26*^{tdTomato}). For sympathetic innervation labeling, we performed whole mount immunostaining with the sympathetic nerve marker Tyrosine Hydroxylase (TH). We then performed whole mount confocal imaging and 3D analysis with Imaris to construct the parasympathetic innervation of the cardiac ventricles together with sympathetic nerves (**Figure 3**).

Surprisingly, the P7 hearts of the *ChATCre;Rosa26*^{tdTomato} mice showed extensive parasympathetic innervation of the ventricles (**Figures 3A$_{i\text{-}ii}$**). Parasympathetic and sympathetic patterning was equally distributed throughout the heart. Moreover, both parasympathetic and sympathetic nerve fibers were intertwined in large bundles, as well as closely localized in smaller axon projections (**Figures 3A$_{ii}$-A$_{iii}$**). We then asked whether both parasympathetic and sympathetic nerve axons extend sequentially, with one guiding the other, or simultaneously, maintaining equal distribution. To investigate this, we used the *ChATCre;Rosa26*^{tdTomato} mice and harvested hearts during developmental stages of axon extension at E15.5 to E17.5 (**Figure 3B, Figure S2**). At E16.5, the axons first reach the apex and demonstrate that parasympathetic and sympathetic nerves are intertwined (**Figures 3B$_{i\text{-}ii}$**). Both parasympathetic and sympathetic nerves pattern together during earlier (E15.5) and later stages (E17.5 and P1) of heart development (**Figure S2**). No differences in distribution were seen on the posterior or anterior side of the heart (**Figure 3, Figure S3**).

To further quantify parasympathetic and sympathetic nerve patterning during embryonic and postnatal development, we used 3D reconstruction and analysis of individual branch trees, primary axons, and whole innervation networks (**Figures 3C-D, Figures S4**). Branching level, density, diameter, and patterning of parasympathetic and sympathetic nerves were investigated

independently. No significant differences were found between the two, therefore we continue to describe the overall patterns identified. We analyzed branching level as a parameter of nerve development (**Figures 3C-D**). A primary axon can branch into secondary-, tertiary-, quintenary axons, and beyond, with each level assigned as branch level 1, 2, 3, respectively. The branching level increased during embryonic and early postnatal development (**Figures 3C-D**). When axons first arise around E15.5, axons have minimal branching level (approx. branch level of 2.5) and mature by P7, with a significant increase in branching level (approx. branch level of 9) (**Figure 3D**). The nerve networks also showed an increase in overall axon distances from origin, max diameter of primary filaments, and primary filament length, with a consistent trend of significance between E17.5 and P7 hearts. (**Figure S4**). Interestingly, the mature heart showed primary and secondary axons were significantly higher density compared to the tertiary branched axons and beyond (**Figure 3E, Figure S4**). These patterns identify two phases of significant nerve growth that occurs between late embryonic and early postnatal development, marked by an increase in axon branch level, distance from origin, max diameter of primary filaments, and length of primary filaments.

Our results demonstrate that parasympathetic nerves extensively innervate the cardiac ventricles and share nearly identical patterning to sympathetic nerves. This architecture is a result of synchronous parasympathetic and sympathetic axon extension, with nerve axons maintaining similar increases in branching level, distribution, and density during heart development.

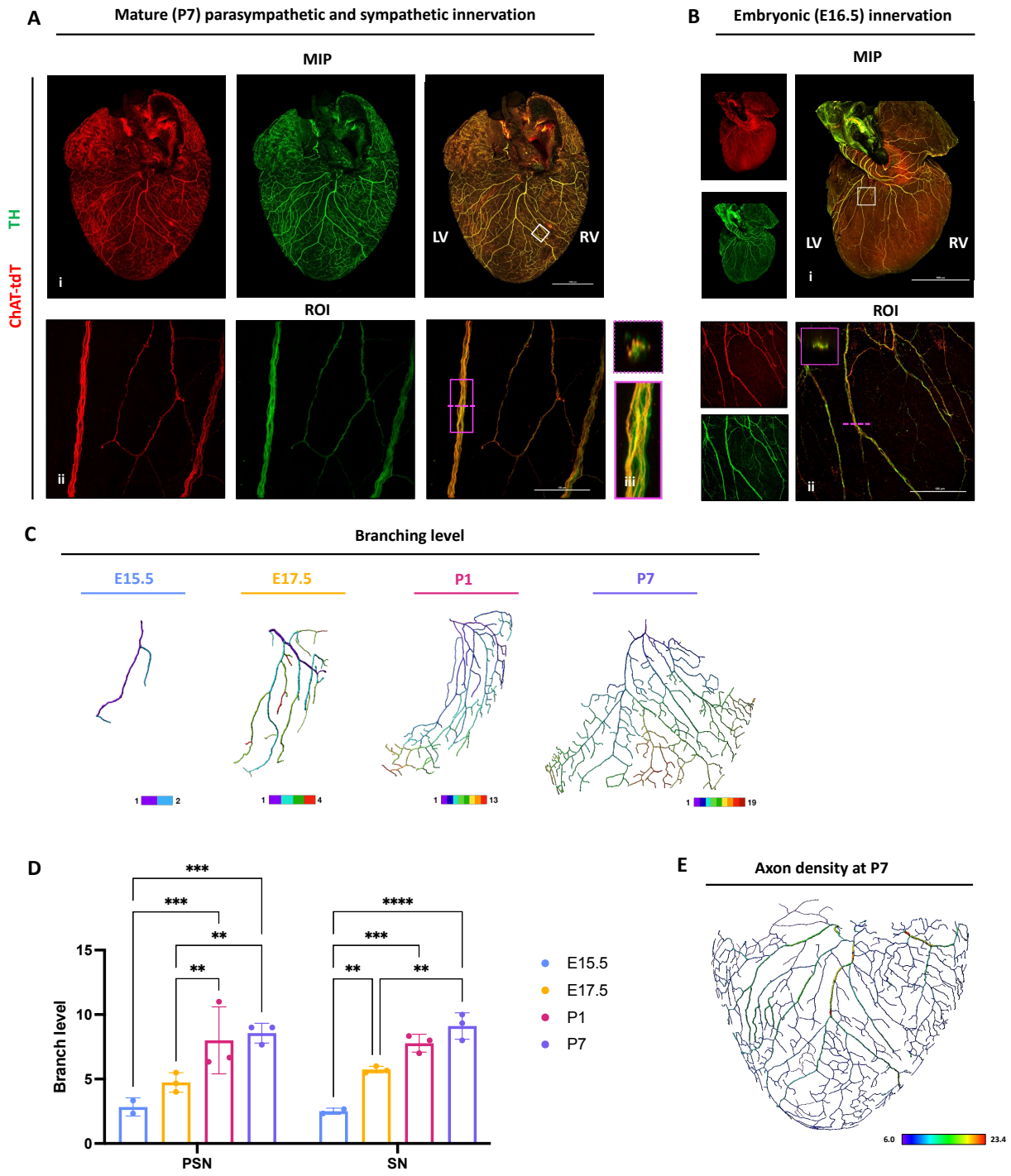

Figure 3. Parasympathetic and sympathetic nerves are bundled and synchronous in development. Parasympathetic reporter hearts (*ChATCre;Rosa26*^{tdTomato}) were immunostained for sympathetic nerves (tyrosine hydroxylase, TH), imaged with confocal microscopy, and

reconstructed with Imaris. (A) The mature nerve patterning shows (A_i) close association between parasympathetic and sympathetic nerves, with (A_{ii}) large and small nerve fibers closely aligned and the (A_{iii}) large axons are bundled (n=5). (B) At E16.5, both parasympathetic and sympathetic axons extend together and are closely localized (n=6). (C-D) 3D modeling and analysis shows increased branching level during embryonic and postnatal development (n=3). (E) Density analysis of the P7 heart shows axon bundles of primary and secondary axons are at higher density than tertiary and higher branched axons.

Reinnervation of the Regenerating Heart and Reestablishment of Nerve-Artery Association

Within a week after birth, the neonatal mouse heart transitions from being highly regenerative into a state of limited regenerative potential. A myocardial infarction (MI) in the non-regenerative heart causes pathological nerve remodeling, resulting in an arrythmia prone heart [26, 27]. In contrast, the neonatal heart can fully regenerate by 21 days-post MI, with full restoration of contractile and autonomic function [32], suggesting that physiological reinnervation may take place during regeneration. Additionally, the regenerative response depends on nerve signaling [31]. Interestingly, regeneration is also dependent on collateral artery formation, where collateral arteries form at 4 days post-MI to bridge the occluded left coronary artery with the right coronary artery and mediate successful cardiac regeneration [34]. During development, artery formation precedes innervation and arterial cells recruit nerve axons to the myocardium [13, 38]. Thus, we hypothesized that newly formed collateral arteries can recruit nerve axons during cardiac regeneration.

To investigate differences in nerve remodeling in the regenerative and diseased, we performed MI surgery in regenerative (P1) or non-regenerative (P7) *Cx40CreER;Rosa26^{tdTomato}* mice and

collected hearts at 7- or 21 days-post MI. Hearts underwent tissue clearing (**Figure 4A**), followed by whole mount immunostaining with the pan-neuronal marker Tuj1 (**Figure 4**). We first investigated innervation remodeling in the non-regenerated heart (**Figure 4B**). We demonstrate that the non-regenerated heart is starkly denervated in the infarct zone at 21 days post-MI (**Figure 4B**). This is similar to the denervation seen in the infarcted adult human heart [39] and interestingly, the degree of denervation, rather than infarction size, is an accurate predictor of ventricular arrhythmias [40] . We then investigated how this compared to nerve remodeling in the regenerative heart. Since collateral arteries are formed by 4 days post-MI in the regenerating heart [34], we began by investigating nerve remodeling shortly after at 7 days post-MI (**Figure 4C**). Interestingly, whole mount imaging demonstrates that although collateral arteries start to appear in the infarct zone at P4, the infarct zone remains denervated at P7 (**Figure 4C**). We then explored the remodeling of nerve-artery architecture in the fully regenerated myocardium at 21 days post-MI (**Figures 4D)**. Our results demonstrate extensive reinnervation of the regenerated myocardium (**Figure 4D$_i$**). Excitingly, the nerves show reestablishment of nerve-artery connection with the collateral arteries, suggesting targeted innervation takes place (**Figure 4D$_{ii}$**).

To determine whether reinnervation is dependent on collateral artery formation, we impaired collateral artery formation using the *Cx40CreER;Cxcr4$^{fl/fl}$* mouse [34] (**Figures 4E-G**). Cxcr4 is a chemokine receptor expressed in arterial endothelial cells that responds to the chemotactic ligand Cxcl12 [41-43]. The Cxcl12/Cxcr4 axis is important for arterial cell migration and artery formation during development and regeneration, where deletion of *Cxcr*4 using the *Cx40CreER* mice impairs collateral artery formation during neonatal heart regeneration [34]. We injected *Cx40CreER;Cxcr4$^{fl/fl}$* pups at P0 with a single dose of tamoxifen and MI was performed within the regenerative window

at P2 (**Figure 4E**). Hearts were collected at 21 days-post-MI and underwent whole-mount clearing and immunostaining for Tuj1. Strikingly, the infarcted area was denervated**,** in stark contrast to the regenerating wild type controls (**Figure 4F-G**), demonstrating that reinnervation is dependent on collateral artery formation. This is the first evidence of targeted reinnervation in the regenerating myocardium, and that this reinnervation is dependent on collateral artery formation.

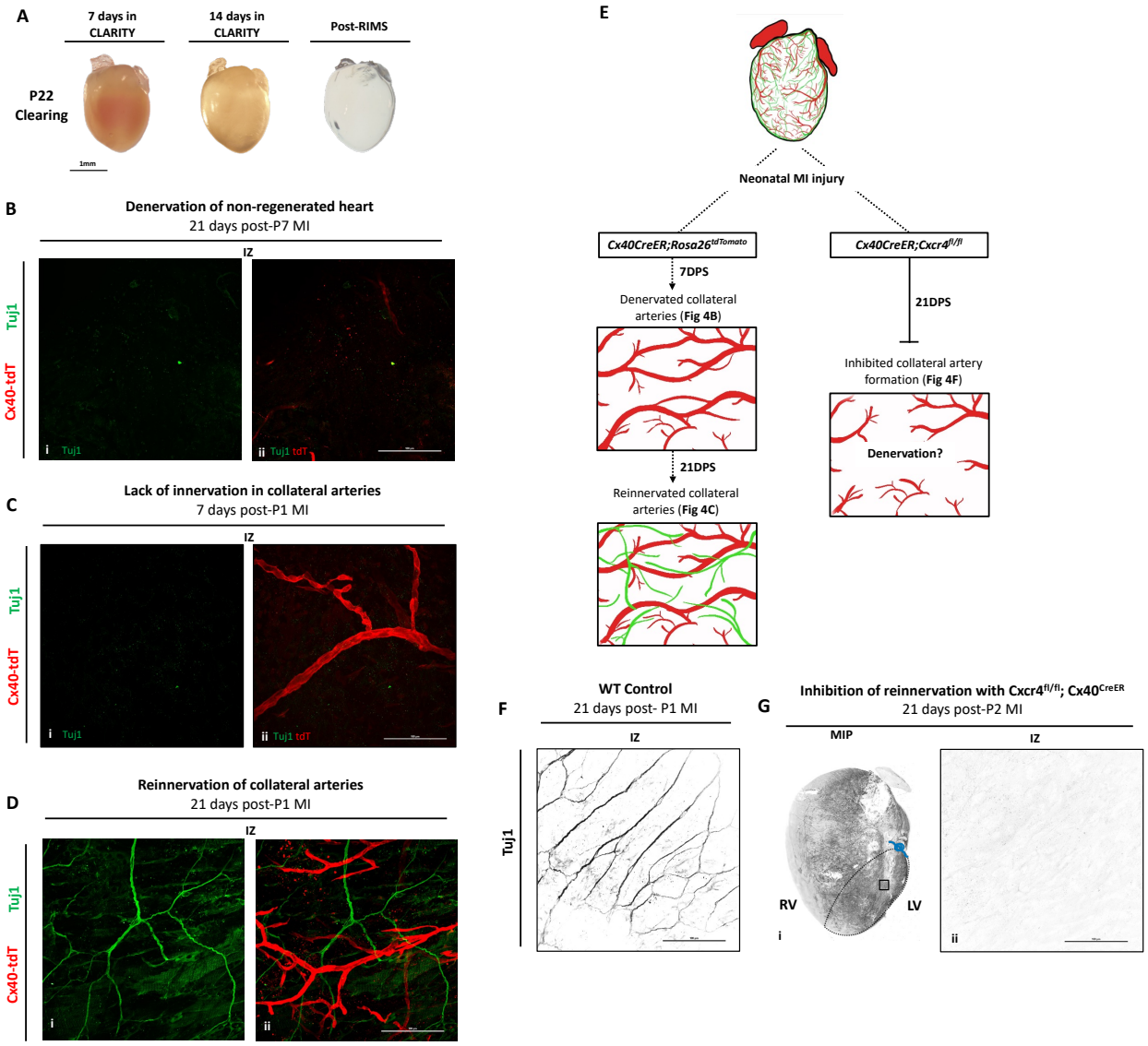

Figure 4. Reinnervation of the regenerating heart is dependent on collateral artery formation. MI was performed in *Cx40CreER;Rosa26*^{tdTomato} mice during the regenerative window (P1 or P2) and hearts were collected at 7- or 21-days post-MI. (A) Hearts underwent tissue clearing

and nerve immunostaining with Tuj1. (B_{i-ii}) 7 days after P1 MI, (B_i) the infarct zone (IZ) is denervated, (B_{ii}) including the newly formed collateral arteries (n=6). (C_{i-ii}) At 21 days after P1 MI, (C_i) the regenerated tissue is reinnervated, (C_{ii}) with nerves showing artery association (n=4). (D) To determine whether reinnervation during regeneration is dependent on collateral artery formation, we used the *Cx40CreER;Cxcr4*$^{fl/fl}$ mouse to inhibit migration of arterial cells post-MI. (F_{i-ii}) At 21 days post-MI, Tuj1 immunostaining showed the IZ remained denervated in the *Cx40CreER;Cxcr4*$^{fl/fl}$ mice (n=4), in comparison to (E) control regenerating hearts (n=4). Black dashed border indicates the IZ and the blue represents the suture site.

Physiological Reinnervation of the Regenerated Myocardium

Nerve remodeling following cardiac injury in the adult mammalian heart is a prominent hallmark of the pathology of heart failure. In contrast, following a neonatal mouse heart injury, the heart regenerates normally, and our results demonstrate reinnervation of the regenerating myocardium. This suggests that reinnervation patterns following adult injury and during neonatal heart regeneration vary widely, and proper innervation patterning is crucial for survival and restoring normal autonomic function of the heart.

To distinguish between nerve remodeling in regenerating and non-regenerating hearts, we performed MI surgery in *ChATCre; Rosa26*^{tdTomato} mice at the regenerative (P1) and non-regenerative (P7) timepoints and collected hearts at 21 days post-MI. Collected hearts were further stained with tdTomato and TH to identify both parasympathetic and sympathetic nerve patterning, respectively. The control uninjured hearts at P22 demonstrate both parasympathetic and sympathetic nerve bundling, and patterning as expected (**Figure 5A**). In contrast, the infarct zone

of the P7 non-regenerating heart at 21 days post-MI showed complete denervation (**Figure 5B$_{iii}$**). Furthermore, the non-regenerating hearts demonstrate sympathetic nerve hyperinnervation at the border zone, a distinctive feature of pathological nerve remodeling (**Figures 5B$_{ii}$**) [29]. Remarkably, the regenerating myocardium at 21 days post-MI of the P1 heart show restoration of both parasympathetic and sympathetic nerve architecture (**Figures 5C$_{i-iii}$**), and the border zone shows large axon bundles of parasympathetic and sympathetic nerves (**Figure 5C$_{ii}$**). This reinnervation of the parasympathetic and sympathetic nerves covers the newly regenerated myocardium (**Figure 5C$_{iii}$**). Collectively, the reestablishment of parasympathetic and sympathetic nerves (**Figure 5C**) along with direct artery reinnervation (**Figure 4C**) demonstrates that physiological reinnervation takes place during regeneration. This is in stark contrast to the non-regenerating heart, which shows denervation of the infarct zone and pathological reinnervation, including sympathetic hyperinnervation at the border zone.

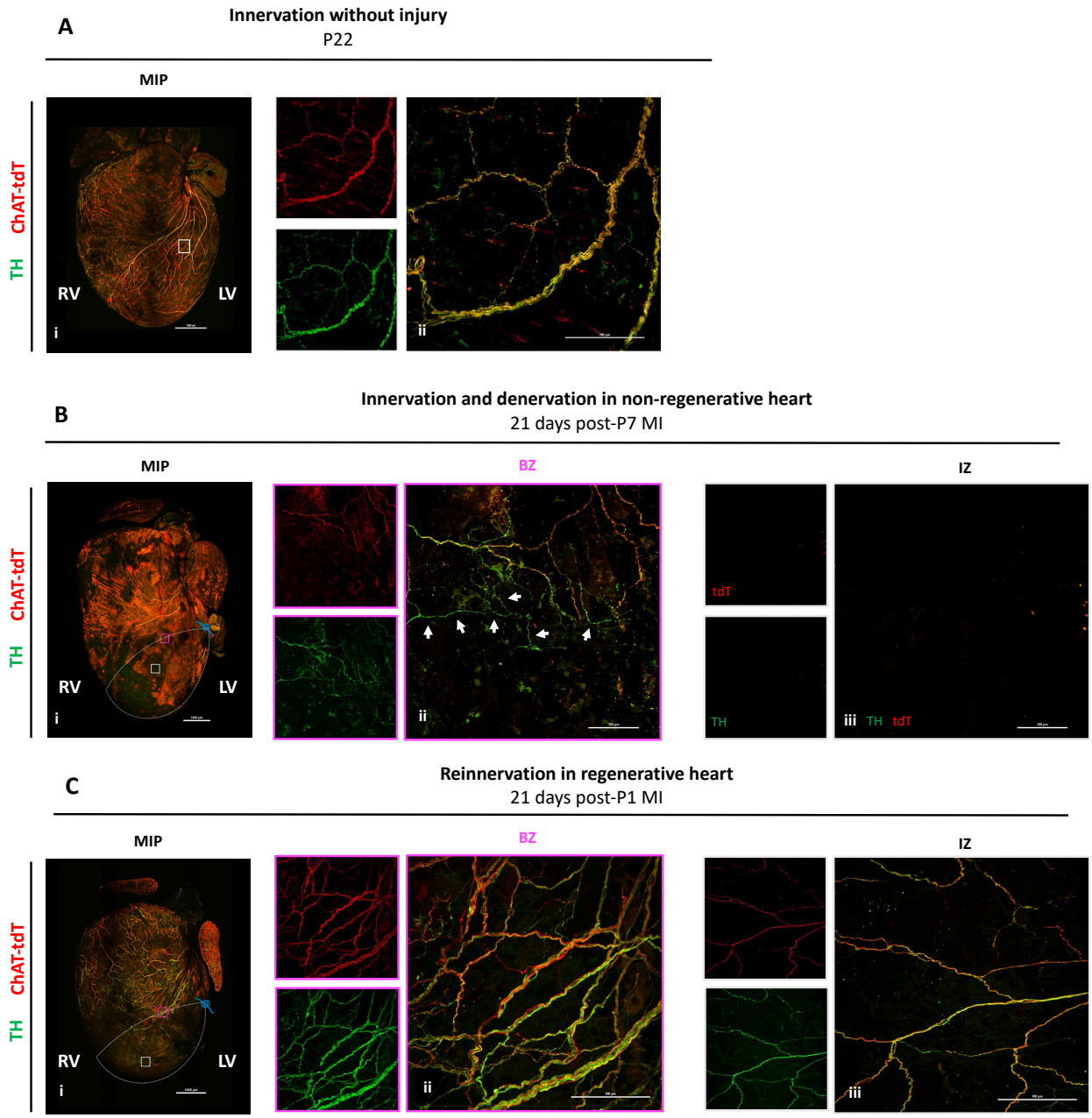

Figure 5. Parasympathetic and sympathetic nerves reinnervate the regenerated myocardium. Myocardial Infarction (MI) was performed on *ChATCre;Rosa26*^{tdTomato} mice at regenerative (P1) and non-regenerative (P7) timepoints. Hearts collected at 21 days post-MI, and immunostained for tyrosine hydroxylase (TH) and imaged with confocal microscopy. ($A_{i=ii}$) Uninjured hearts in adult (P22) mice show parasympathetic and sympathetic nerve entanglement in (A_i) whole mount and (A_{ii}) in the medial region of the myocardium (n=6). ($B_{i=iii}$) Non-

regenerating hearts show pathological remodeling of the nerves. (B_{ii}) The border zone (BZ) shows reinnervation of sympathetic axons, independent of parasympathetic axons. (B_{iii}) The infarct zone (IZ) is denervated (n=6). ($C_{i=iii}$) The regenerated heart shows reestablished parasympathetic and sympathetic axon bundling. (C_{ii}) The BZ shows large nerve bundles of both nerve subtypes. (C_{iii}) The IZ shows reinnervation of parasympathetic and sympathetic axons (n=5). White dashed border indicates the IZ and the blue represents the suture site.

DISCUSSION

Neural regulation of the cardiovascular system has been recognized for a long time, however; the importance of neurocardiology in cardiovascular health and disease is beginning to be appreciated. Recent studies aimed at identifying the cellular and molecular makeup of the intrinsic cardiac nervous system and the sinoatrial node underscore the importance of elucidating the innervation patterns and function of different parts of the cardiac nervous system [4, 5]. Sympathetic innervation of cardiac ventricles has been studied extensively [6, 13], however; parasympathetic innervation has been underappreciated due to technical limitations [16]. In our experience, whole mount immunolabeling of ChAT is technically challenging. Furthermore, 2D analysis from histological sections is inaccurate and cannot reconstruct the complex patterns of nerves and networks with other cell types. Furthermore, endogenous labeling using a lineage reporter alone is prone to quenching (**Figure S5**). To overcome this limitation, we utilized the *ChATCre; Rosa26*^{tdTomato} model together with whole mount immunostaining for tdTomato and tissue clearing, which allowed for an accurate view of the parasympathetic nervous system. Our finding of extensive parasympathetic innervation of the ventricles indicates potential intracellular dynamics and physiological influences between parasympathetic nerves and the surrounding heart tissue.

Furthermore, we demonstrate a spatiotemporal innervation pattern of cardiac ventricles with respect to coronary veins and arteries.

Cardiac injury results in neuronal degeneration and pathological nerve remodeling, which leads to a disruption in heart innervation patterns [26, 27, 29]. This neural remodeling and pathological innervation that occurs following injury leads to fatal arrhythmias [25]. Nerves have been therapeutically targeted using neuromodulation approaches, such as vagal nerve stimulation and sympathetic nerve denervation [44-47]. Some studies demonstrate promising outcomes, however; our lack of understanding of cardiac nerve development and remodeling hampers our understanding of the mechanisms by which these approaches modulate reinnervation and function [48].

Neonatal mice can regenerate their hearts following injury for a brief window after birth [32]. Cardiac nerves have been demonstrated to regulate cardiomyocyte proliferation and neonatal heart regeneration [31]. Furthermore, autonomic heart functions are restored following regeneration, suggesting that physiological reinnervation take place, which contrasts with the pathological innervation that takes place following adult cardiac injury. Additionally, from a clinical perspective, it has been well established that heart transplant recipients receive a completely de-innervated heart, which eventually becomes partially innervated by the host [49]. Thus, understanding the development and plasticity of cardiac innervation is a unique approach to stimulate physiological innervation and cardiac regeneration.

Remarkably, we demonstrate for the first time the reestablishment of physiological innervation of the regenerating myocardium, suggesting that this reinnervation likely preserves autonomic

function of the regenerated myocardium in contrast to the non-regenerating hearts. Furthermore, we demonstrate that physiological innervation is dependent on collateral artery formation, where inhibition of collateral arteries following injury blocks this reinnervation. These results suggest that promoting collateral artery formation can be targeted to promote both physiological reinnervation and cardiac regeneration following injury.

Our study reveals new insights into cardiac innervation during development, disease, and regeneration. However, it remains unclear whether a distinct gene regulatory network mediates physiological and pathological innervation. Furthermore, identifying the signals by which coronary arteries regulate reinnervation during regeneration can play an important role in treatment of autonomic dysfunction, as well as promote cardiac repair following injury. Our results provide a framework to start dissecting the cellular and molecular networks that guide cardiac innervation and regeneration.

Acknowledgments

Funding for this project was provided by an AHA Predoctoral Fellowship 829586 (R.J.S.), NIH/NHLBI R56 HL155617 (A.I.M.), NIH/NHLBI R01 HL166256 (A.I.M.), DOD W81XWH2210094 (A.I.M.), and NIH/NIGMS R35 GM 134865 (A.A.). We thank Lucile Miquerol and Kristy Red-Horse for generously sharing the *Cx40CreER* mice. We thank Lance Rodenkirch and the Optical Imaging Core (Grant 1S10OD025040-01) for imaging support.

Declaration of interests

The authors declare no competing interests.

REFERENCES

1. Hasan W. Autonomic cardiac innervation: development and adult plasticity. *Organogenesis*. 2013;9:176-193.
2. Randall WC. *Nervous control of cardiovascular function*: Oxford University Press, USA; 1984.
3. Randall WC. *Nervous control of the heart*: Williams and Wilkins Company; 1965.
4. Achanta S, Gorky J, Leung C, Moss A, Robbins S, Eisenman L, Chen J, Tappan S, Heal M, Farahani N, Huffman T, England S, Cheng ZJ, Vadigepalli R and Schwaber JS. A Comprehensive Integrated Anatomical and Molecular Atlas of Rat Intrinsic Cardiac Nervous System. *iScience*. 2020;23:101140.
5. Hanna P, Dacey MJ, Brennan J, Moss A, Robbins S, Achanta S, Biscola NP, Swid MA, Rajendran PS, Mori S, Hadaya JE, Smith EH, Peirce SG, Chen J, Havton LA, Cheng ZJ, Vadigepalli R, Schwaber J, Lux RL, Efimov I, Tompkins JD, Hoover DB, Ardell JL and Shivkumar K. Innervation and Neuronal Control of the Mammalian Sinoatrial Node a Comprehensive Atlas. *Circ Res*. 2021;128:1279-1296.
6. Vegh AMD, Duim SN, Smits AM, Poelmann RE, Ten Harkel ADJ, DeRuiter MC, Goumans MJ and Jongbloed MRM. Part and Parcel of the Cardiac Autonomic Nerve System: Unravelling Its Cellular Building Blocks during Development. *J Cardiovasc Dev Dis*. 2016;3.
7. Zaglia T and Mongillo M. Cardiac sympathetic innervation, from a different point of (re)view. *J Physiol*. 2017;595:3919-3930.
8. Dokshokova L, Franzoso M, Di Bona A, Moro N, Sanchez Alonso JL, Prando V, Sandre M, Basso C, Faggian G, Abriel H, Marin O, Gorelik J, Zaglia T and Mongillo M. Nerve growth factor transfer from cardiomyocytes to innervating sympathetic neurons activates TrkA receptors at the neuro-cardiac junction. *J Physiol*. 2022;600:2853-2875.
9. Larrivée B, Freitas C, Suchting S, Brunet I and Eichmann A. Guidance of vascular development: lessons from the nervous system. *Circ Res*. 2009;104:428-41.
10. Habecker BA, Anderson ME, Birren SJ, Fukuda K, Herring N, Hoover DB, Kanazawa H, Paterson DJ and Ripplinger CM. Molecular and cellular neurocardiology: development, and cellular and molecular adaptations to heart disease. *J Physiol*. 2016;594:3853-75.
11. Hildreth V, Anderson RH and Henderson DJ. Autonomic innervation of the developing heart: origins and function. *Clin Anat*. 2009;22:36-46.
12. Moon JI and Birren SJ. Target-dependent inhibition of sympathetic neuron growth via modulation of a BMP signaling pathway. *Dev Biol*. 2008;315:404-17.
13. Nam J, Onitsuka I, Hatch J, Uchida Y, Ray S, Huang S, Li W, Zang H, Ruiz-Lozano P and Mukouyama YS. Coronary veins determine the pattern of sympathetic innervation in the developing heart. *Development*. 2013;140:1475-85.
14. Tampakakis E, Gangrade H, Glavaris S, Htet M, Murphy S, Lin BL, Liu T, Saberi A, Miyamoto M, Kowalski W, Mukouyama YS, Lee G, Minichiello L and Kwon C. Heart neurons use clock genes to control myocyte proliferation. *Sci Adv*. 2021;7:eabh4181.
15. Pianca N, Di Bona A, Lazzeri E, Costantini I, Franzoso M, Prando V, Armani A, Rizzo S, Fedrigo M, Angelini A, Basso C, Pavone FS, Rubart M, Sacconi L, Zaglia T and Mongillo M. Cardiac sympathetic innervation network shapes the myocardium by locally controlling cardiomyocyte size through the cellular proteolytic machinery. *J Physiol*. 2019;597:3639-3656.

16. Coote JH. Myths and realities of the cardiac vagus. *J Physiol*. 2013;591:4073-85.
17. Dunlap ME, Bibevski S, Rosenberry TL and Ernsberger P. Mechanisms of altered vagal control in heart failure: influence of muscarinic receptors and acetylcholinesterase activity. *Am J Physiol Heart Circ Physiol*. 2003;285:H1632-40.
18. Mittmann C, Pinkepank G, Stamatelopoulou S, Wieland T, Nürnberg B, Hirt S and Eschenhagen T. Differential coupling of m-cholinoceptors to Gi/Go-proteins in failing human myocardium. *J Mol Cell Cardiol*. 2003;35:1241-9.
19. Brack KE, Winter J and Ng GA. Mechanisms underlying the autonomic modulation of ventricular fibrillation initiation--tentative prophylactic properties of vagus nerve stimulation on malignant arrhythmias in heart failure. *Heart Fail Rev*. 2013;18:389-408.
20. Nalivaiko E, Antunes VR and Paton JF. Control of cardiac contractility in the rat working heart-brainstem preparation. *Exp Physiol*. 2010;95:107-19.
21. Johnson TA, Gray AL, Lauenstein JM, Newton SS and Massari VJ. Parasympathetic control of the heart. I. An interventriculo-septal ganglion is the major source of the vagal intracardiac innervation of the ventricles. *J Appl Physiol (1985)*. 2004;96:2265-72.
22. Rysevaite K, Saburkina I, Pauziene N, Vaitkevicius R, Noujaim SF, Jalife J and Pauza DH. Immunohistochemical characterization of the intrinsic cardiac neural plexus in whole-mount mouse heart preparations. *Heart Rhythm*. 2011;8:731-8.
23. Pauza DH, Saburkina I, Rysevaite K, Inokaitis H, Jokubauskas M, Jalife J and Pauziene N. Neuroanatomy of the murine cardiac conduction system: a combined stereomicroscopic and fluorescence immunohistochemical study. *Auton Neurosci*. 2013;176:32-47.
24. Yasuhara O, Matsuo A, Bellier JP and Aimi Y. Demonstration of choline acetyltransferase of a peripheral type in the rat heart. *J Histochem Cytochem*. 2007;55:287-99.
25. Fukuda K, Kanazawa H, Aizawa Y, Ardell JL and Shivkumar K. Cardiac innervation and sudden cardiac death. *Circ Res*. 2015;116:2005-19.
26. Cao JM, Chen LS, KenKnight BH, Ohara T, Lee MH, Tsai J, Lai WW, Karagueuzian HS, Wolf PL, Fishbein MC and Chen PS. Nerve sprouting and sudden cardiac death. *Circ Res*. 2000;86:816-21.
27. Cao J-M, Fishbein MC, Han JB, Lai WW, Lai AC, Wu T-J, Czer L, Wolf PL, Denton TA, Shintaku IP, Chen P-S and Chen LS. Relationship Between Regional Cardiac Hyperinnervation and Ventricular Arrhythmia. *Circulation*. 2000;101:1960-1969.
28. Li W, Knowlton D, Van Winkle DM and Habecker BA. Infarction alters both the distribution and noradrenergic properties of cardiac sympathetic neurons. *Am J Physiol Heart Circ Physiol*. 2004;286:H2229-36.
29. Yokoyama T, Lee JK, Miwa K, Opthof T, Tomoyama S, Nakanishi H, Yoshida A, Yasui H, Iida T, Miyagawa S, Okabe S, Sawa Y, Sakata Y and Komuro I. Quantification of sympathetic hyperinnervation and denervation after myocardial infarction by three-dimensional assessment of the cardiac sympathetic network in cleared transparent murine hearts. *PLoS One*. 2017;12:e0182072.
30. Kumar A and Brockes JP. Nerve dependence in tissue, organ, and appendage regeneration. *Trends in Neurosciences*. 2012;35:691-699.
31. Mahmoud AI, O'Meara CC, Gemberling M, Zhao L, Bryant DM, Zheng R, Gannon JB, Cai L, Choi WY, Egnaczyk GF, Burns CE, Burns CG, MacRae CA, Poss KD and Lee RT. Nerves Regulate Cardiomyocyte Proliferation and Heart Regeneration. *Dev Cell*. 2015;34:387-99.

32. Porrello ER, Mahmoud AI, Simpson E, Hill JA, Richardson JA, Olson EN and Sadek HA. Transient regenerative potential of the neonatal mouse heart. *Science*. 2011;331:1078-80.
33. Miquerol L, Thireau J, Bideaux P, Sturny R, Richard S and Kelly RG. Endothelial plasticity drives arterial remodeling within the endocardium after myocardial infarction. *Circ Res*. 2015;116:1765-71.
34. Das S, Goldstone AB, Wang H, Farry J, D'Amato G, Paulsen MJ, Eskandari A, Hironaka CE, Phansalkar R, Sharma B, Rhee S, Shamskhou EA, Agalliu D, de Jesus Perez V, Woo YJ and Red-Horse K. A Unique Collateral Artery Development Program Promotes Neonatal Heart Regeneration. *Cell*. 2019;176:1128-1142 e18.
35. Mahmoud AI, Porrello ER, Kimura W, Olson EN and Sadek HA. Surgical models for cardiac regeneration in neonatal mice. *Nat Protoc*. 2014;9:305-311.
36. Salamon RJ, Zhang Z and Mahmoud AI. Capturing the Cardiac Injury Response of Targeted Cell Populations via Cleared Heart Three-Dimensional Imaging. *JoVE*. 2020:e60482.
37. Mao S, Xiong G, Johnson BN, Cohen NA and Cohen AS. Blocking Cross-Species Secondary Binding When Performing Double Immunostaining With Mouse and Rat Primary Antibodies. *Front Neurosci*. 2021;15:579859.
38. Su T, Stanley G, Sinha R, D'Amato G, Das S, Rhee S, Chang AH, Poduri A, Raftrey B, Dinh TT, Roper WA, Li G, Quinn KE, Caron KM, Wu S, Miquerol L, Butcher EC, Weissman I, Quake S and Red-Horse K. Single-cell analysis of early progenitor cells that build coronary arteries. *Nature*. 2018;559:356-362.
39. Ripplinger CM, Noujaim SF and Linz D. The nervous heart. *Prog Biophys Mol Biol*. 2016;120:199-209.
40. Fallavollita JA, Heavey BM, Luisi AJ, Jr., Michalek SM, Baldwa S, Mashtare TL, Jr., Hutson AD, Dekemp RA, Haka MS, Sajjad M, Cimato TR, Curtis AB, Cain ME and Canty JM, Jr. Regional myocardial sympathetic denervation predicts the risk of sudden cardiac arrest in ischemic cardiomyopathy. *J Am Coll Cardiol*. 2014;63:141-9.
41. Ivins S, Chappell J, Vernay B, Suntharalingham J, Martineau A, Mohun TJ and Scambler PJ. The CXCL12/CXCR4 Axis Plays a Critical Role in Coronary Artery Development. *Dev Cell*. 2015;33:455-68.
42. Chang AH, Raftrey BC, D'Amato G, Surya VN, Poduri A, Chen HI, Goldstone AB, Woo J, Fuller GG and Dunn AR. DACH1 stimulates shear stress-guided endothelial cell migration and coronary artery growth through the CXCL12–CXCR4 signaling axis. *Genes & development*. 2017;31:1308-1324.
43. Cavallero S, Shen H, Yi C, Lien C-L, Kumar SR and Sucov HM. CXCL12 signaling is essential for maturation of the ventricular coronary endothelial plexus and establishment of functional coronary circulation. *Developmental cell*. 2015;33:469-477.
44. Vaseghi M, Gima J, Kanaan C, Ajijola OA, Marmureanu A, Mahajan A and Shivkumar K. Cardiac sympathetic denervation in patients with refractory ventricular arrhythmias or electrical storm: intermediate and long-term follow-up. *Heart Rhythm*. 2014;11:360-6.
45. Sharma K, Premchand RK, Mittal S, Monteiro R, Libbus I, DiCarlo LA, Ardell JL, Amurthur B, KenKnight BH and Anand IS. Long-term Follow-Up of Patients with Heart Failure and Reduced Ejection Fraction Receiving Autonomic Regulation Therapy in the ANTHEM-HF Pilot Study. *Int J Cardiol*. 2021;323:175-178.

46. Bourke T, Vaseghi M, Michowitz Y, Sankhla V, Shah M, Swapna N, Boyle NG, Mahajan A, Narasimhan C, Lokhandwala Y and Shivkumar K. Neuraxial modulation for refractory ventricular arrhythmias: value of thoracic epidural anesthesia and surgical left cardiac sympathetic denervation. *Circulation*. 2010;121:2255-62.
47. Hadaya J and Ardell JL. Autonomic Modulation for Cardiovascular Disease. *Front Physiol*. 2020;11:617459.
48. Brandt EB, Bashar SJ and Mahmoud AI. Stimulating ideas for heart regeneration: the future of nerve-directed heart therapy. *Bioelectron Med*. 2019;5:8.
49. Bravo PE, Lautamaki R, Carter D, Holt DP, Nekolla SG, Dannals RF, Russell SD and Bengel FM. Mechanistic Insights into Sympathetic Neuronal Regeneration: Multitracer Molecular Imaging of Catecholamine Handling After Cardiac Transplantation. *Circ Cardiovasc Imaging*. 2015;8:e003507.